Journal of
Medicinal Chemistry

Article

Tideglusib and its analogs as inhibitors of Staphylococcus aureus SrtA

Teng Yang, Tao Zhang, Xiangna Guan, Ze Dong, Le-Fu Lan, Song Yang, and Cai-Guang Yang

J. Med. Chem., **Just Accepted Manuscript** • DOI: 10.1021/acs.jmedchem.0c00803 • Publication Date (Web): 08 Jul 2020

is published by the American Chemical Society. 1155 Sixteenth Street N.W., Washington, DC 20036

Tideglusib and its analogs as inhibitors of *Staphylococcus aureus* SrtA

Teng Yang[†,‡,§], Tao Zhang[‡,§], Xiang-Na Guan[‡,¶], Ze Dong[‡], Lefu Lan[‡,¶,Δ], Song Yang[†,*], Cai-Guang Yang[‡,¶,Δ*]

[†] State Key Laboratory Breeding Base of Green Pesticide and Agricultural Bioengineering, Key Laboratory of Green Pesticide and Agricultural Bioengineering, Ministry of Education, Center for R&D of Fine Chemicals, Guizhou University, Guizhou 550025, China

[‡] State Key Laboratory of Drug Research, Shanghai Institute of Materia Medica, Chinese Academy of Sciences, Shanghai 201203, China

[¶] University of the Chinese Academy of Sciences, Beijing 100049, China

[Δ] School of Pharmaceutical Science and Technology, Hangzhou Institute for Advanced Study, UCAS, Hangzhou 310024, China

[§] These authors contributed equally to this work

*Correspondence: jhzx.msm@gmail.com (S.Y.) or yangcg@simm.ac.cn (C.-G.Y.)

ABSTRACT

Sortase A (SrtA) anchors surface proteins to the cell wall envelope, and it has attracted increasing interesting as a potential antivirulence target. Several small-molecule inhibitors for SrtA have been developed, but target validation remains largely underexplored. Herein, we report a new class of SrtA inhibitors that supports antivirulence therapy through small-molecule targeting of SrtA. Tideglusib

(**TD**), a drug candidate for myotonic dystrophy, was outstanding in high-throughput screening. A concise synthetic route quickly provided **TD** analogs, and the structure-activity relationships for SrtA inhibition have been established from those analogs. Several compounds largely retained the *in vitro* potency and exhibited a better solubility than **TD**. Additionally, **TD** attenuated virulence-related phenotypes *in vitro* and protected mice against lethal *S. aureus* USA300 bacteremia. Our study indicates that **TD** and its analogs could be new candidates as SrtA inhibitors with potential in the development of new antivirulence agents.

Key words: *S. aureus,* tideglusib, antivirulence, sortase A, inhibitor.

INTRODUCTION

Staphylococcus aureus is a major gram-positive pathogenic bacteria that causes serious suppurative infection of tissues as well as pneumonia and sepsis.[1] Antibiotics, either bactericidal or bacteriostatic, are widely used clinically for antiinfective therapy .[2] However, the inappropriate use and abuse of antibiotics have led to the emergence of drug-resistant bacteria, such as methicillin-resistant *S. aureus* (MRSA), which is the most common cause of the nosocomial infections and difficult to treat due to resistance against many different drugs.[3-6] In order to alleviate antimicrobial resistance, the continued research for new antibiotics is necessary. In addition, antibacterial drug discovery should highlight the needs for new antiinfective agents, particularly those with new modes of action, such as antivirulence compounds.[7-11]

The sortase A (SrtA) transpeptidase is a biologically proven target ideal for the development of antivirulence drugs.[12, 13] Genome sequencing revealed that all *S. aureus* isolates encode 17-21 surface proteins with LPXTG sorting signals, which fulfill diverse functions in the development of pathogenesis.[14, 15] Without these surface proteins anchored on the cell wall, the bacteria display low virulence. SrtA specifically recognizes and incorporates these surface proteins on the cell wall envelope using active-site cysteine biochemistry.[15] The *srtA* mutant lost its function in assembling surface proteins into the envelope and was unable to trigger bacteremia or sepsis in mice,[12, 16] but it is not essential for bacterial viability. Additionally, SrtA is a membrane enzyme that is much more easily accessible.

Recent research efforts have been directed at developing antivirulence therapies against *S. aureus*, focusing on small-molecule inhibitors for sortase which interferes with assembly of surface proteins.[17] These inhibitors can be grouped into three classes based on the resources of the compounds: natural products,[18-23] synthetic small molecules,[24-29] and substrate-derived peptides.[30-33] On the basis of their mode of action, SrtA inhibitors can be classified into two groups, covalent and noncovalent inhibitors.[34, 35] Covalent inhibitors react with the active-site cysteine to form a covalent bond,[36, 37] whereas noncovalent inhibitors bind reversibly to SrtA. While these studies identified both competitive and non-competitive inhibitors, many SrtA inhibitors exhibited moderate potency, undetermined cytotoxicity, and unknown *in vivo* antiinfective activity. Even worse, some SrtA inhibitors diminished or blocked staphylococcal growth, which indicated that they are not selective inhibitors of the

sortase enzyme. Therefore, it has not been fully established whether the SrtA protein could be chemically attenuated for antivirulence therapy against *S. aureus*.

Herein, we report the screening and structure-activity relationship (SAR) study of tideglusib and its analogs as the inhibitors of *S. aureus* SrtA.

RESULTS AND DISCUSSION

High-throughput screening (HTS) for SrtA inhibitors. Previously, we developed a reversible SrtA inhibitor (sodium 3-(3-(pyridin-4-yl)-[1,2,4]triazolo[3,4-*b*][1,3,4]thiadiazol-6-yl)benzenesulfonate, **6e**) that may be a useful antiinfective therapeutic to prevent *S. aureus* infection without the side effects of antibiotics (Figure S1). [38] In addition to demonstrating antiinfective efficacy *in vivo*, to our knowledge, this is the first inhibitor that has been shown to inhibit the sortase-mediated cleavage of surface-protein sorting signals *in vivo*. To search for new inhibitors of *S. aureus* SrtA, we performed HTS on a compound library consisting of 2,400 clinical drugs and candidates using fluorescence resonance energy transfer (FRET) to measures the transpeptidation activity of recombinant $SrtA_{\Delta N24}$ on a fluorogenic peptide substrate (Abz-LPATG-Dnp).[15] In addition to the FRET-based assay, the inhibitory activities of the hit compounds were further validated by an orthogonal PAGE-based method we previously established, in which the surface protein $IsdA_{64-323}$ was assayed as an $SrtA_{\Delta N24}$ substrate to rule out interference from false-positive effects of fluorogenic compounds.[38]

Interestingly, tideglusib (**TD**) was outstanding in the initial FRET-based HTS (Figure 1), and it efficiently inhibited SrtA-mediated transpeptidation on the protein substrate in the PAGE-based assay. **TD** has been granted fast-track designation for the treatment of congenital myotonic dystrophy and orphan drug designation for myotonic dystrophy type 1.[39] In addition, the thiadiazolidinone scaffold in **TD** has been demonstrated as an efficient pharmacophore in drug discovery for Alzheimer's disease,[40] although in-depth SAR investigations remain largely underexplored. These data highlight the excellent drug-like properties of **TD**, which make this promising chemical space for the development of SrtA inhibitors.

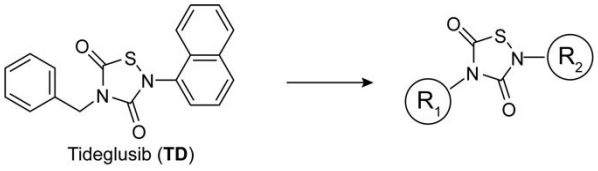

Figure 1. Screening hit **TD** provides a chemical scaffold for new inhibitors of SrtA.

Synthesis of TD analogs. To explore the SARs of the new set of SrtA inhibitors, we performed a concise synthesis of **TD** and its analogs by incorporating different substituents (R_1 and R_2) into the core structure of **TD** (Figure 1 and Scheme 1).[41] Commercially available isothiocyanates **1** were mixed with isocyanates **2** in the presence of sulfuryl chloride at 0 °C; then, the reaction was warmed to rt. Resulting intermediate S-chloroisothiocarbamoyl chlorides **3** were further transformed *in situ* to provide **TD** and analogs **TD1**-**TD31** in good yields. Generally, commercially unavailable isocyanate **2'** was prepared from 3,5-dimethylisoxazol-4-amine **4** by reaction with triphosgene, and **2'** was then reacted with different isothiocyanates **1**

to afford analogs **TD32**-**TD40**. The concise synthetic route made it possible to quickly evaluate the effects of R_1 and R_2 on the SrtA inhibitory activities.

Scheme 1. General synthesis of TD and its analogs.

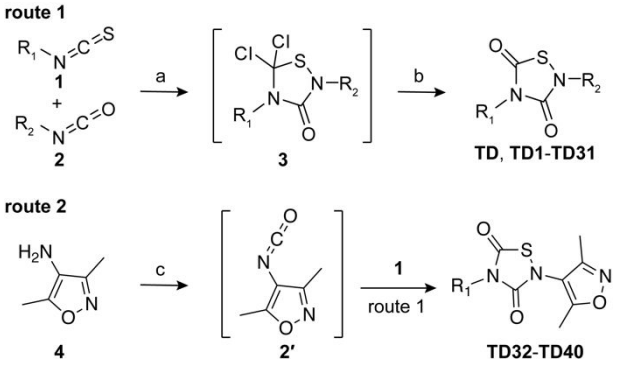

Conditions: (a) SO_2Cl_2, THF, 0 °C-rt, overnight; (b) air, 30 min; (c) triphosgene, THF, 50 °C, 1 hr.

SAR analysis. The inhibitory activities of the designed analogs were evaluated by both FRET-based and PAGE-based assays on $SrtA_{\Delta N24}$ transpeptidation of peptide and protein substrates, and the results are given as FRET IC_{50} and PAGE IC_{50}, respectively (Table 1). Although a small IC_{50} values were usually observed in the FRET-based assay, we suggest that PAGE IC_{50} is more meaningful than FRET IC_{50} as fewer compounds interfere with the IC_{50} value in the PAGE-based assay. We also monitored the minimal inhibitory concentration (MIC) to rule out the bactericidal or bacteriostatic compounds because the ideal inhibitors for SrtA should have minimal impacts on bacterial viability. Indeed, **TD** and several analogs minimally inhibited the growth of the *S. aureus* Newman strain at concentrations up to 100 μg/mL (Table 1), which might indicate that **TD** analogs would be unlikely to function in the same manner as conventional antibiotics.

Table 1. Effects of substituted benzyl substituents at R_1

Comp.	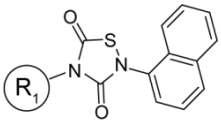	FRET IC_{50} (μM)[a]	PAGE IC_{50} (μM)[b]	MIC (μg/mL)[c]	cLogP[d]
TD	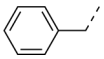	0.6 ± 0.2	5.9 ± 0.1	>100.0	5.2
TD1	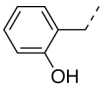	1.3 ± 0.2	32.2 ± 0.7	>100.0	4.6
TD2	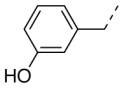	1.6 ± 0.3	9.2 ± 0.3	>100.0	4.6
TD3	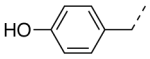	2.6 ± 0.2	4.7 ± 0.8	100.0	4.6
TD4	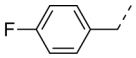	4.1 ± 0.2	5.9 ± 1.1	100.0	5.4
TD5	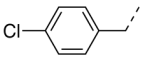	0.7 ± 0.3	23.1 ± 0.3	100.0	5.9
TD6	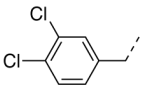	0.9 ± 0.1	14.4 ± 0.1	50.0	6.5
TD7	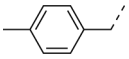	1.2 ± 0.2	12.6 ± 0.7	100.0	5.1

[a] Measured by monitoring the cleavage of a fluorogenic peptide substrate (Abz-LPATG-Dnp) by $SrtA_{\Delta N24}$ in a FRET-based assay. [b] Measured by monitoring the transpeptidation of $IsdA_{64-323}$ by $SrtA_{\Delta N24}$ in a PAGE-based assay. [c] Against growth of the *S. aureus* Newman strain. [d] Predicted in ChemBioDraw Professional 14.

First, we kept the naphthalene ring constant to explore the effect of the functionality on the benzyl group in R_1 for SrtA inhibition. As shown in Table 1, the introduction of hydroxyl substituents (**TD1-TD3**) appeared to lower compound cLogP in comparison to that for **TD**, while slightly attenuated the SrtA inhibitory activity measured in the

FRET-based assay. However, the position of the hydroxy moiety on the phenyl ring dramatically alters the SrtA inhibitory activity in the PAGE-based assay. Compounds **TD3** and **TD4** bearing hydroxy or fluoro substituents at the para-position of the phenyl ring largely retain the activity of **TD**, as observed in the PAGE-based assay. Introducing chloro or methyl substituents to the phenyl ring gave analogs **TD5-TD7**, which exhibited weaker inhibition of $SrtA_{\Delta N24}$, as detected in the PAGE-based assay. Taken together, the substituents on the benzyl group were further altered to prepare more analogs, which displayed inhibitory activities comparable to that of the parent compound, **TD**.

Next, we explored whether the incorporation of more flexible alkyl chains as the R_1 group could affect the inhibitory activity of the $SrtA_{\Delta N24}$ inhibitors. As shown in Table 2, the one or two carbon-long alkyl substituents in compounds **TD8** or **TD9** are favorable and result in the lower cLogP values. Although all the tested compounds, including **TD10** and **TD11**, bearing larger or bulky alkyl groups retained the inhibitory activity for the $SrtA_{\Delta N24}$ enzyme, as observed in the FRET-based assay, the moderate activity detected in the PAGE-based assay implies that flexible substituents in the R_1 positions are not favorable.

Table 2. SAR of TD derivatives bearing flexible alkyl substituents at R_1

Comp.	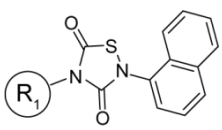	FRET IC_{50} (μM)[a]	PAGE IC_{50} (μM)[b]	MIC (μg/mL)[c]	cLogP[d]
TD8	H_3C	0.8 ± 0.2	8.0 ± 0.3	100.0	3.4

TD9		0.7 ± 0.3	8.2 ± 0.1	>100.0	4.0
TD10		0.9 ± 0.2	12.6 ± 0.8	100.0	5.0
TD11	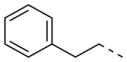	0.6 ± 1.1	27.5 ± 1.0	>100.0	5.5

[a,b,c,d] Same definitions used as in Table 1.

Given that the bulky naphthalene might generally make the **TD** derivatives too rigid for SrtA binding, we fixed R_2 as a benzyl group and prepared a new set of derivatives by varying the substituents at the R_1 position (Table 3). A short alkyl group at position R_1, typically less than four carbons, improves lipid-water partition coefficient; for example, consider compounds **TD12**, **TD14** and **TD15**. Those derivatives of **TD** bearing a benzyl group at the R_2 position and an aliphatic substituent in R_1 showed dramatically decreased activity, as detected in both assays, such as compound **TD12-TD14**. Similarly, compounds **TD17**-**TD20**, with two benzyl substituents, showed significantly decreased inhibitory activities as $SrtA_{\Delta N24}$ inhibitors. Moreover, the introduction of sterically bulky groups at R_1, such as isopropyl (**TD15**) and fluorophenyl (**TD16**), abolished the $SrtA_{\Delta N24}$ inhibitory activity. Additionally, all **TD** analogs bearing a benzyl group at the R_2 position displayed increased activity against the growth of the *S. aureus* Newman strain *in vitro* with moderate MIC values, which indicates that these analogs do not truly function as SrtA inhibitors. Consistently, the thiadiazolidinedione derivatives were previously identified to function as antibiotics through selectively inhibiting bacterial dihydroorotate dehydrogenase (DHODH), which is a critical enzyme in *de novo*

pyrimidine biosynthesis in prokaryotic and eukaryotic cells.[42] However, it remains underexplored whether the bactericidal activities of our **TD** analogs could also likely be attributed to the selective inhibition of bacterial DHODH. Taken together, we observed that all the tested derivatives bearing a benzyl groups at R_2 exhibited decreased inhibitory activity toward SrtA and inhibited bacterial growth unanticipatedly, which emphasizes the contribution of the rigid aromatic moiety at the R_2 position.

Table 3. SAR of TD derivatives with benzyl groups at R_2

Comp.	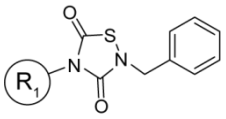	FRET IC_{50} (μM)[a]	PAGE IC_{50} (μM)[b]	MIC (μg/mL)[c]	cLogP[d]
TD12		3.5 ± 1.5	23.6 ± 0.2	12.5	2.3
TD13		8.4 ± 0.3	21.2 ± 0.8	6.2	3.9
TD14		2.0 ± 0.5	16.7 ± 0.5	25.0	2.9
TD15		>100	>50.0	6.2	3.1
TD16	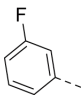	>100	>50.0	12.5	4.2
TD17	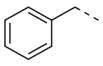	7.0 ± 0.2	12.9 ± 0.3	12.5	4.1
TD18	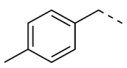	5.1 ± 4.0	35.7 ± 2.6	12.5	4.6
TD19	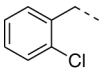	3.4 ± 0.8	28.0 ± 1.1	12.5	4.8
TD20	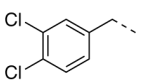	2.9 ± 1.3	19.7 ± 0.1	12.5	5.4

[a,b,c,d] Same definitions used as in Table 1.

We then explored the incorporation of more flexible R_2 groups (Table 4). The aliphatic groups in R_2 are unfavorable for inhibition since none of the synthesized compounds (**TD21**-**TD28**) showed enzymatic inhibition of $SrtA_{\Delta N24}$ in either assays. These analogs with an aliphatic R_2 moiety displayed even better bactericidal activity than did the analogs bearing a benzyl group at the R_2 position (Table 3), which is consistent with the previous observation that aliphatic and/or benzyl substituted thiadiazolidinones could function as antibiotics.[43] These data, alongside the SAR observations listed in Table 3, indicate that rigid R_2 substituents are likely important for SrtA inhibition by **TD** analogs.

Table 4. SAR of TD derivatives bearing flexible alkyl substituents at both positions

Comp.	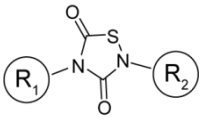	FRET IC_{50} (μM)[a]	PAGE IC_{50} (μM)[b]	MIC (μg/mL)[c]	cLogP[d]
TD21	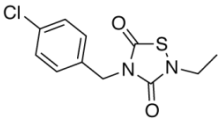	8.7 ± 0.9	>50.0	6.2	3.5
TD22	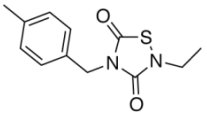	16.7 ± 2.4	>50.0	6.2	3.3
TD23	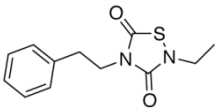	16.3 ± 0.9	>50.0	6.2	3.1
TD24	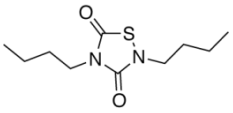	43.9 ± 1.4	>50.0	3.1	3.7
TD25	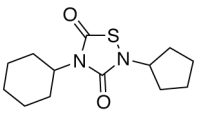	10.2 ± 0.6	>50.0	6.2	4.0

TD26	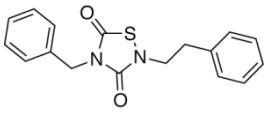	10.1 ± 0.5	42.7 ± 3.2	12.5	4.4
TD27	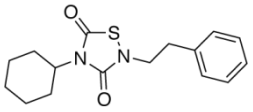	>100	>50.0	12.5	4.6
TD28	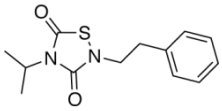	>100	>50.0	25.0	3.5

[a,b,c,d] Same definitions used as in Table 1.

According to the SAR analysis above, a benzyl substituent at R_1 is favorable for $SrtA_{\Delta N24}$ inhibition activity, while analogs with alkyl groups in R_2 exhibited decreased inhibitory activity. Next, we sought to investigate the effects of different aromatic R_2 groups on $SrtA_{\Delta N24}$ inhibition when R_1 was fixed as a benzyl group (Table 5). Both **TD29** and **TD32** remained highly active compared to **TD**, and minimally impaired the viability of the *S. aureus* Newman strain. It should be highlighted that **TD32** might exhibit improved solubility after introducing heterocycle moiety compared to that of **TD**. Indeed, the solubility of **TD32** was estimated to be 144 μg/mL in phosphate-buffered saline (PBS) in the presence of 1% DMSO, while the solubility of **TD** is about 11 μg/mL. The derivatives bearing benzocycloalkanes, compounds **TD30** and **TD31**, were much less active than **TD**. These data further support the necessity of having an aromatic substituent at the R_2 position for SrtA inhibition.

Table 5. Effect of R_2 when R_1 is a benzyl group

Comp.		FRET IC_{50} (μM)[a]	PAGE IC_{50} (μM)[b]	MIC (μg/mL)[c]	cLogP[d]

TD29		3.4 ± 0.2	4.7 ± 0.2	>100.0	4.0
TD30		4.4 ± 0.4	45.6 ± 2.1	>100.0	5.0
TD31	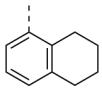	6.0 ± 0.2	31.9 ± 1.6	50.0	5.6
TD32		0.8 ± 0.1	4.6 ± 0.1	>100.0	3.0

[a,b,c,d] Same definitions applied as in Table 1.

Last, we fixed R_2 as the motif derived from **TD32**, and then explored the effects of different substituents at R_1 on the inhibition of $SrtA_{\Delta N24}$. As shown in Table 6, in general, the alkyl group in R_1 influenced the $SrtA_{\Delta N24}$ inhibition. Compounds with short aliphatic chains, such as compounds **TD33** and **TD34**, largely retained the activity against $SrtA_{\Delta N24}$ transpeptidation in both assays, while compound **TD35**, with a sterically bulky group, made the **TD** analog inactive for $SrtA_{\Delta N24}$ inhibition. For derivatives bearing substituted benzyl groups at the R_1 position, the presence of methyl, methoxy, or chloro substituents on the phenyl ring of **TD32**, such as in compounds **TD36**-**TD40**, resulted in activities comparable to that of compound **TD32**. In addition, the MIC data show that these analogs are inactive against *S. aureus in vitro*, which indicates that the **TD32** analogs might not function as traditional antibiotics for treating infection. Taken together, several analogs bearing a 3,5-dimethylisoxazole substituent at R_2 position exhibited good inhibitory activity on $SrtA_{\Delta N24}$.

Table 6. SAR of R_1 with the R_2 motif derived from TD32

Comp.	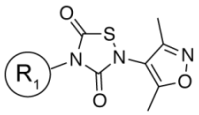	FRET IC_{50} (μM)[a]	PAGE IC_{50} (μM)[b]	MIC (μg/mL)[c]	cLogP[d]
TD33		1.5 ± 0.3	6.3 ± 0.3	>100.0	1.8
TD34		1.1 ± 0.1	4.1 ± 1.0	>100.0	2.8
TD35		12.6 ± 0.1	>50.0	>100.0	2.1
TD36		1.1 ± 0.1	4.7 ± 0.2	>100.0	3.5
TD37		1.2 ± 0.1	5.0 ± 0.2	>100.0	2.9
TD38		0.9 ± 0.1	3.4 ± 0.1	>100.0	4.3
TD39		0.6 ± 0.4	3.7 ± 0.5	>100.0	3.7
TD40		1.0 ± 0.4	4.1 ± 0.5	>100.0	3.7

[a,b,c,d] Same definitions applied as in Table 1.

TD and analogs are reversible inhibitors of SrtA and are not PAINS-containing. **TD** is an irreversible inhibitor of glycogen synthase kinase-3β (GSK-3β),[44] and a derivative of **TD** covalently binds to regulators of G protein signaling protein 4 by forming a disulfide bond.[45] Additionally, a **TD** analog was found to effectively inactivate bacterial DHODH enzymes regardless of the presence of cysteine residues in their primary structures.[46] However, **TD** compounds do not inhibit cysteine protease papain.[41, 45] The covalent modification of cysteine residues is thus unlikely to be the general mechanism of action for **TD** compounds, but they might depend on the environment in the binding site of the target. We investigated whether **TD** and its

analog function as covalent inhibitors for SrtA transpeptidation. Using ESI-LC/MS analysis, $SrtA_{\Delta N24}$ was determined at an m/z of 22967.5 Da (Figure 2A), while a 120.5 Da m/z shift was observed after $SrtA_{\Delta N24}$ was incubated with the generic covalent alkylator, *N*,*N*,*N*-trimethyl-2-[(methylsulfonyl)sulfanyl]ethanaminium bromide (**MTSET**) as a positive control at rt for 12 hr (Figures 2B and S1), and this shift in mass perfectly matched to the fragment of **MTSET** covalently added to $SrtA_{\Delta N24}$. No m/z shift was observed when $SrtA_{\Delta N24}$ was exposed to either the **TD** or **TD32** inhibitor under the same conditions as used for the control groups (Figures 2C and 2D), which revealed that **TD** compounds could not covalently modify the $SrtA_{\Delta N24}$ protein *in vitro*. However, whether they covalently modify SrtA in cells remains unclear. Next, we measured the recovery of sortase activity in a reversible inhibition assay that has been published.[38] As shown in Figure 2E, the covalent alkylator **MTSET** abolished the transpeptidation activity of $SrtA_{\Delta N24}$, while this activity was mostly recovered in the groups of treating with **TD** inhibitors and following dilution of $SrtA_{\Delta N24}$/inhibitor at 10 fold IC_{50} as compared to mock treated $SrtA_{\Delta N24}$, which indicate that **TD** and **TD32** are reversible inhibitors. More generally, a time-dependent increase in the apparent inhibitory potency suggests irreversible binding. The inhibition effects of **TD** and **TD32** on $SrtA_{\Delta N24}$ minimally changed over time (Figure S2A). Taken together, the **TD** inhibitors inhibit the transpeptidation in a reversible manner.

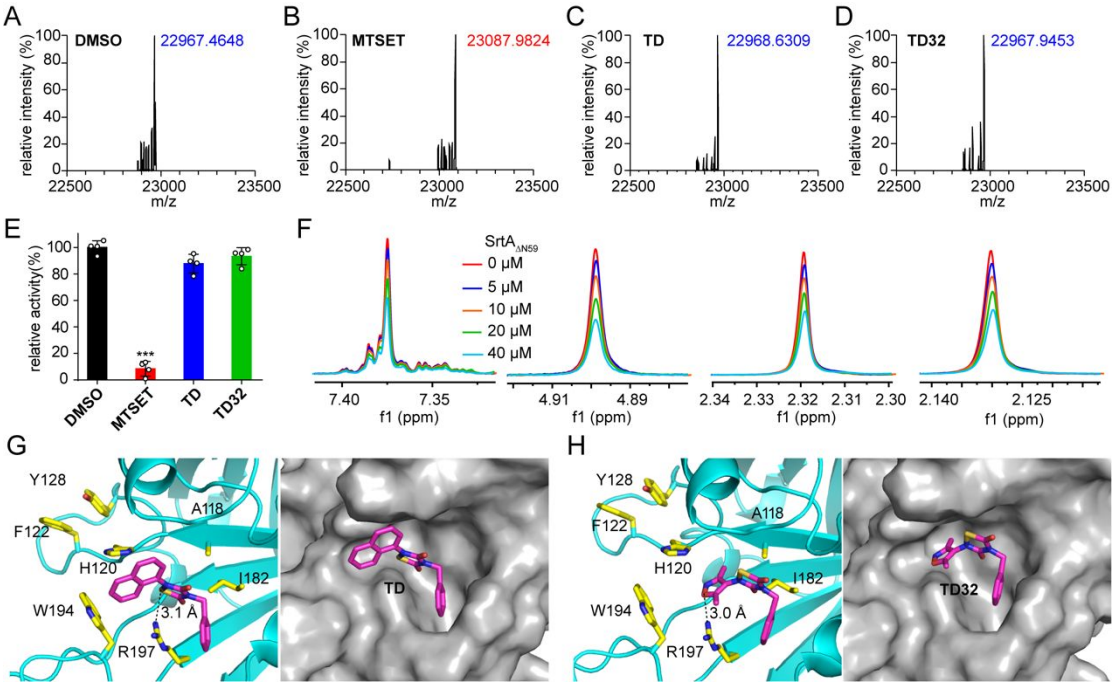

Figure 2. Characterization on the mode of actions of the **TD** inhibitors. MS analysis of $SrtA_{\Delta N24}$ protein treated with DMSO (A), the covalent alkylator **MTSET** (B), the inhibitor **TD** (C), and the inhibitor **TD32** (D). (E) Determination of the reversibility of the $SrtA_{\Delta N24}$ inhibition. Two independent experiments were performed. (F) NMR spectra of **TD32** interacting with the $SrtA_{\Delta N59}$ protein. The CPMG-NMR spectra were recorded for **TD32** without $SrtA_{\Delta N59}$ (red) and with $SrtA_{\Delta N59}$ at 5.0 μM (blue), 10.0 μM (magenta), 20.0 μM (green), and 40.0 μM (cyan). Two independent experiments were performed. Docking of **TD** (G) and **TD32** (H) to the solution structure of $SrtA_{\Delta N59}$ (PDB code ID: 2KID) performed in AutoDock 4.2. Protein is shown as a cartoon in cyan, the surface is presented in gray, the side chains are in yellow, and the inhibitors are in magenta.

We further investigated the interactions between SrtA and the **TD** inhibitors. Since the solution structure of $SrtA_{\Delta N59}$ bound with peptide has been determined,[47] we

performed Carr-Purcell-Meiboom-Gill (CPMG) nuclear magnetic resonance (NMR) titrations by using the $SrtA_{\Delta N59}$ truncation. Dose-dependent attenuation of the signals was observed in CPMG NMR titrations (Figures 2F), which suggested direct interactions between $SrtA_{\Delta N59}$ and the inhibitor **TD32**. When $SrtA_{\Delta N24}$ was incubated in 10-fold excesses of **TD** and **TD32**, we observed no obvious changes in the circular dichroism (CD) spectra (Figure S2B), which means **TD** and its derivatives cause no gross structural perturbations in SrtA folding.[48] Additionally, we performed a docking study to reveal the potential binding modes between the **TD** inhibitors and $SrtA_{\Delta N59}$ (Figures 2G and 2H). Both inhibitors could bind in the substrate binding pocket of SrtA. The naphthyl ring of **TD** forms a π-π stacking with His120. A hydrogen bond forms between the sulfur atom in **TD** and the side chain of Arg197 in $SrtA_{\Delta N59}$, while the 3,5-dimethylisoxazole ring in **TD32** forms a hydrogen bond with the side chain of Arg197. These observed differences in hydrogen-binding modes might explain why the heterocycle of thiadiazolidinedione posed differently in binding to **TD** and **TD32**. In the docked pose of the inhibitors binding to $SrtA_{\Delta N59}$, the methylene of the benzyl group is close to the Ile182 residue in SrtA, which is a constrained position for introducing more or bulkier substituents. This is consistent with the experimental observations that analogs with bulky groups, for example, isopropyl (**TD15**, **TD28** and **TD35**), fluorophenyl (**TD16**) and cyclohexyl (**TD25** and **TD27**), at R_1 showed no inhibitory activities. There is space in the benzyl group binding pocket for the binding of an extra substituent, which also explains why the introduction of methyl (**TD36**),

methoxy (**TD37**), or chloro (**TD38**-**TD40**) moieties on the phenyl ring minimally affected the inhibitory activity on SrtA transpeptidation.

Furthermore, we investigated whether **TD** compounds are PAINS-containing inhibitors of SrtA.[49, 50] **TD** and **TD32** are not intrinsically fluorescent (Figure S2C). If their inhibitory activities are attenuated by small amounts of nonionic detergent, the inhibitors are likely aggregators. The presence of 0.01% v/v freshly prepared Triton X-100 minimally affected the inhibitory activities of **TD** and **TD32** in a typical FRET-based assay (Figure S2D). These data suggest that the **TD** compounds are not PAINS-containing inhibitors of SrtA.

Determination of the enzymatic activity of SrtA inhibitors. After filtration of the PAINS properties, we chose **TD** and **TD32** for further investigations as SrtA inhibitors, while the covalent inhibitor **MTSET** was assayed as a positive control, and compound (*E*)-3-phenyl-5-(2-(phenylsulfonyl)vinyl)-2-(propylamino)-4a,8a-dihydronaphthalene-1,4-dione (**63**) was assayed as a negative control (Figure S1).[36] Both **TD** and **TD32** efficiently inhibited the cleavage of the fluorogenic peptide substrate (Abz-LPATG-Dnp) by $SrtA_{\Delta N24}$ in a concentration-dependent manner, and their IC_{50} values were calculated to be 0.6 μM and 0.8 μM, respectively (Figure 3A). **TD32** also inhibited the transpeptidation of $IsdA_{64-323}$ protein by $SrtA_{\Delta N24}$ in a dose-dependent manner, and its activity was comparable to that of **TD** (Figure 3B). Deletion of the *srtA* gene minimally attenuated the *in vitro* growth of the *S. aureus* Newman strain;[12] consistent with this result, neither **TD** nor **TD32** inhibited the growth of the *S. aureus* Newman strain at concentrations up to 100 μM (Figure 3C), while **TD** at 200 μM

attenuated bacterial growth, which means at least it has bacteriostatic properties and therefore is not a true antivirulence inhibitor at this high concentration.

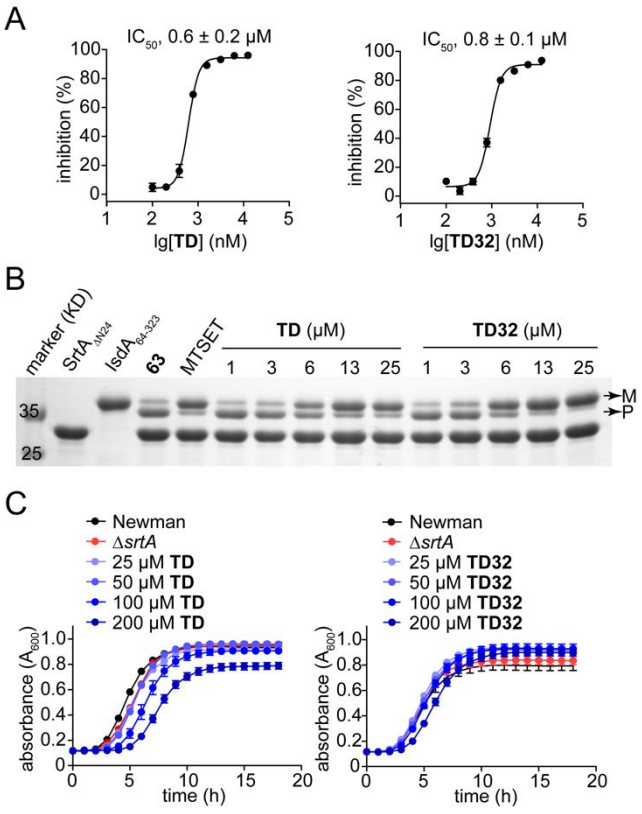

Figure 3. Inhibition of SrtA transpeptidation. (A) Determination of the IC_{50} values of the inhibition of the $SrtA_{\Delta N24}$ enzyme by a FRET-based assay. (B) Effect of the inhibitors on the $SrtA_{\Delta N24}$-mediated transpeptidation of $IsdA_{64\text{-}323}$ protein in PAGE-based assay. The migratory positions of the $IsdA_{64\text{-}323}$ substrate precursor (M) and mature transpeptidation product (P) are indicated. **MTSET** was assayed as a positive control, while **63** was assayed as a negative control. (C) Effects of the inhibitors on the growth of the *S. aureus* Newman strain. The Δ*srtA* mutant *S. aureus* Newman strain was assayed as a positive control. Three independent experiment were performed for these assays.

Effect of the TD inhibitors on virulence-related phenotypes in *S. aureus*. The inhibition of SrtA activity in staphylococci by compounds **TD** and **TD32** was then evaluated. SrtA anchors several surface proteins in the staphylococcal envelope, including SpA.[12, 38, 51-53] Since SpA can specifically bind FITC-labeled human IgG, the abundance of IgG-bound SpA in the bacterial cell wall envelope can be roughly estimated from the fluorescence. In the control assay, the *srtA* deletion mutant *S. aureus* strain almost completely lost its ability to anchor SpA to the cell wall (Figure 4A). The covalent inhibitor **MTSET** reduced the abundance of anchored SpA, while the negative control (**63**) had minimal effect on the abundance of anchored SpA when the *S. aureus* Newman strain was exposed to the test compounds at a concentration of 100 μM. As expected, both **TD** and **TD32** reduced the amount of anchored SpA in a concentration-dependent manner (Figure 4A). The reduction in cell wall-anchored SpA induced by the SrtA inhibitors also could be clearly visualized in the Western blot assay (Figure 4B). Biofilm formation is a critical pathogenic process of *S. aureus*.[54] MRSA biofilms increase its resistance to antimicrobial action from external agents.[5] In this context, the development of strategies to prevent, remove, or disperse biofilms is critical for the treatment of MRSA infections. It has been demonstrated that *srtA* gene deletion or inhibition of the SrtA protein can reduce the ability of in *S. aureus* to form biofilms.[20] To investigate whether **TD** and **TD32** inhibit biofilm formation, we performed a gentian violet staining assay to calculate biofilm biomass. Noncovalent inhibitor **6e** was assayed as a positive control (Figure S1).[38] Compared to the wild-type control groups, a significant decrease in

biofilm biomass was observed when *S. aureus* was exposed to **TD** or **TD32**, and the decreases were dose dependent (Figure 4C). Taken together, the **TD**-derived SrtA inhibitors inhibit virulence-related phenotypes in *S. aureus*.

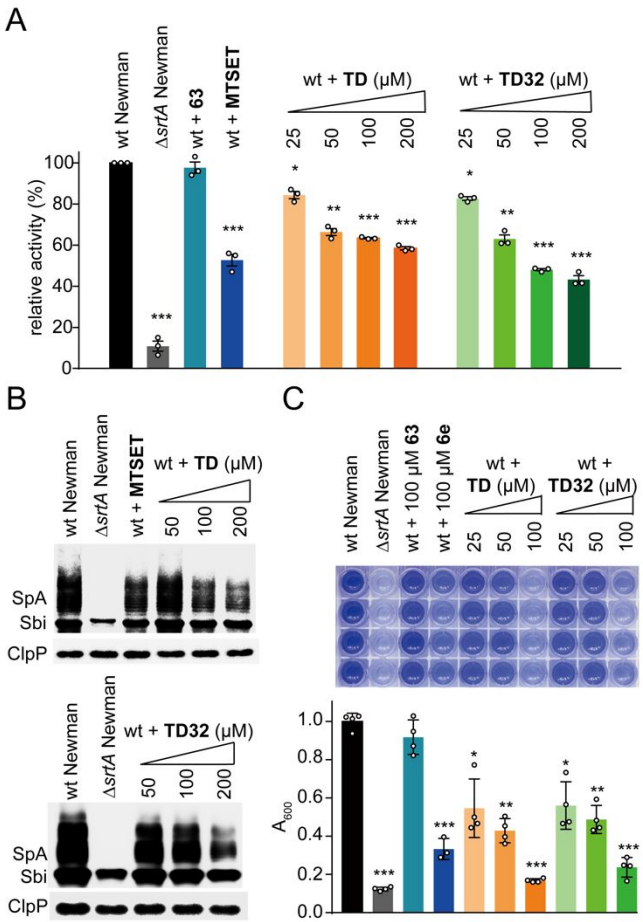

Figure 4. Effect of SrtA inhibitors on virulence-related phenotypes in the *S. aureus* Newman strain. (A) Effects of SrtA inhibitors on cell wall-anchored SpA estimated based on the fluorescence of FITC-labeled human IgG. **MTSET** and the Δ*srtA* mutant *S. aureus* Newman strain were assayed as positive controls, while **63** was used as a negative control. Statistical significance (*, $P < 0.05$; **, $P < 0.01$; ***, $P < 0.001$) was determined using the unpaired, two-tailed Student's t-test (n = 3). (B) Effects of SrtA inhibitors on cell wall-anchored SpA detected by Western blot. The Δ*srtA* mutant *S.*

aureus Newman strain was assayed as a positive control. The Cytoplasmic protein ClpP of *S. aureus* was used as a loading control. The non-specific band of Sbi was indicated. (C) Effects of SrtA inhibitors on biofilm formation in the *S. aureus* Newman strain. The top panel shows a photograph of a biofilm stained with crystal violet, and the bottom panel shows the quantification of biofilm determined by measuring the absorbance at a wavelength of 600 nm. Compound **6e** and the Δ*srtA* mutant *S. aureus* Newman strain were assayed as positive controls, while **63** was assayed as a negative control. Statistical significance (*, $P < 0.05$; **, $P < 0.01$; ***, $P < 0.001$) was determined using the unpaired, two-tailed Student's t-test (n = 4). Three independent experiments were performed for all assays.

Antiinfective therapy with TD. Although **TD32** displayed activity comparable to that of **TD** and better solubility than **TD**, the biosafety of **TD** has already been established since it is a drug candidate undergoing phase II clinical trials for congenital myotonic dystrophy treatment.[39] In addition, the *S. aureus* USA300 strain is a community-associated MASR strain and resistant to many drugs. Therefore, we evaluated the *in vivo* antiinfective efficacy of **TD** against the *S. aureus* USA300 strain. As shown in Figure 5A, **TD** reduced the virulence factor of the *S. aureus* USA300 strain, biofilm formation for example. Also, the inhibitor **TD** at 150 μg/mL slightly attenuated the *in vitro* growth of the tested strain (Figure 5B), which suggested that it is unlikely that **TD** inactivates *S. aureus* by a mechanism similar to those of conventional antibiotics. A previous pharmacokinetic study of **TD** revealed that the postintraperitoneal administration maximum concentrations in plasma were low

since the C_{max} was only 137 ng/mL when a single dose of 10 mg/kg **TD** was administered to mice.[55] Therefore, a high dose of **TD** is necessary to achieve a sufficient high concentration for SrtA inhibition in mouse. The antiinfective properties of **TD** were assessed in a mouse model of systemic infection via i.v. inoculation of 1×10^8 colony-forming units (CFU) of *S. aureus* USA300, which load is a lethal load for healthy mice. As shown in Figure 5C, placebo-treated mice died rapidly on the third day to the sixth day. However, the mice that had received i.p. treatment of compound **TD** at a dose of 40 mg/kg/day displayed a prolonged time to death and 40% survival at the endpoint of monitoring, which showed that the placebo and **TD** had different *in vivo* effects (*, $P < 0.05$). This *in vivo* assessment indicated that the chemical scaffold of **TD** is promising for the development of SrtA inhibitors, which might be useful as antiinfective agents in preventing *S. aureus* bloodstream infections in community-associated settings.

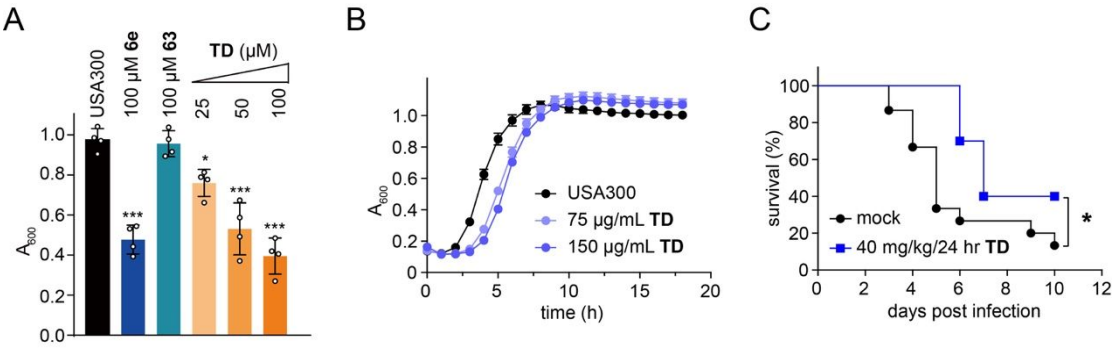

Figure 5. Antiinfective therapy with **TD**. (A) Effects of **TD** on biofilm formation in the *S. aureus* USA300 strain. Compound **6e** was assayed as positive controls, while **63** was assayed as a negative control. Statistical significance (*, $P < 0.05$; ***, $P < 0.001$) was determined using the unpaired, two-tailed Student's t-test (n = 4). Three

independent experiments were performed. (B) Effects of **TD** on the growth of the *S. aureus* USA300 strain. Three independent experiments were performed. (C) Antiinfective effects of **TD** on BALB/c mice (n = 10) infected by the *S. aureus* USA300 strain. The survival rate was recorded over a 10-day period. Statistical significance was examined with the log-rank test (placebo vs. **TD**, $P < 0.05$).

CONCLUSION

Currently, all antibiotics in therapeutic application or in development pipelines are bactericidal or bacteriostatic, which has put pressure on bacteria to evolve resistance. To address the challenge posed by the rapid emergence of new resistance, antibacterial drug discovery should emphasize the need to find new antiinfective agents, particularly those with novel modes of action. Targeting bacterial virulence is one of the most promising strategies, and it represents a complementary or alternative strategy to conventional antibiotics. Sortases and cell wall anchored surface proteins contribute to the virulence of many different Gram-positive bacteria. Thus, antivirulence strategy with sortase inhibitors may be useful to broadly prevent bacterial infections with antibiotic-resistant bacterial pathogens. However, the identification of sortase inhibitors as antiinfective therapeutics has not been fully demonstrated.

In this study, we employed FRET-based HTS on a library consisting of over 2,400 clinical drugs and candidates. **TD** was identified as a hit compound for the *in vitro* inhibition of $SrtA_{\Delta N24}$ in the low micromolar range. Subsequently, an SAR exploration

of SrtA inhibitors was quickly established via the concise synthesis of **TD** analogs. Some analogs are effective inactivators of the growth of *S. aureus*, while others displayed weaker inhibitory activities on the $SrtA_{\Delta N24}$ enzyme. Several analogs bearing the 3,5-dimethylisoxazole moiety retained inhibitory activities comparable to that of **TD** and exhibited solubility superior to that of **TD**. The anchoring of SpA was reduced when *S. aureus* was exposed to **TD** and **TD32**, which also led to the attenuation of biofilm formation. Importantly, **TD** is effective in protecting mice against lethal infection by the *S. aureus* USA300 strain. Whether the potential off-target effect and/or the slight bacteriostatic property of **TD** would influence the observed outcome in mouse infection warrants further study. In summary, **TD** and its analogs represent a new chemical scaffold for SrtA inhibitors, making them promising lead compounds in the development of new antivirulence drugs.

EXPERIMENTAL SECTION

General methods. All chemicals were analytically pure and were used as received. Reactions were monitored by thin-layer chromatography (TLC) using silica gel-coated TLC plates, and detection was performed by UV absorbance at a wavelength of 254 nm. ^{1}H NMR spectra were recorded on a Bruker-400 (400 MHz) spectrometer using DMSO-d_6 or $CDCl_3$ as the solvent. The data are reported as chemical shifts or δ values (ppm). ^{13}C NMR spectra were obtained on a Bruker-500 (125 MHz) spectrometer using DMSO-d_6 or $CDCl_3$ as the solvent. Agilent 1200 (HPLC) and 6110 (MSD) instruments were utilized for generating HPLC traces, obtaining mass spectrometry data, and evaluating purity. The system was equipped with a PDA UV detector and

an Xbridge C18 column (3.5 μm, 4.6 × 50 mm), and the separations were achieved at rt. The HPLC gradient program utilized 5% to 95% MeCN in H_2O with 0.01% trifluoroacetic acid over 5 min with a 1.5 mL/min flow rate. The purity of the final compound was assessed at a wavelength of 254 nm by HPLC analysis. Reversed-phase preparatory purifications were performed on a Lisui EZ Plus 100 D. This system utilized a PDA detector and a Kromat flash C18 column (20-40 μm, 120 g). Purification methods used a 30-min gradient from 5% to 70% MeCN in H_2O. The purity of each target compound was >95% by HPLC.

General synthesis of compounds TD and TD1-TD32. Sulfuryl chloride (238 mg, 2.0 mmol, 1.0 eq) was added into a solution of isothiocyanate (**1**, 1.0 eq) and isocyanate (**2**, 1.0 eq) in anhydrous THF at 0 °C and the mixture was warmed to rt and then stirred for 4-10 hr. The precipitate was separated by filtration and washed with cold THF (2 × 10 mL) and hexane (2 × 10 mL). Alternatively, the reaction mixture was concentrated under vacuum and purified by reversed-phase C18 (RP-C18) column chromatography to give the target compound.

4-benzyl-2-(naphthalen-1-yl)-1,2,4-thiadiazolidine-3,5-dione (**TD**). Obtained in 80% yield; white powder; ^{1}H NMR (400 MHz, $CDCl_3$) δ 8.01 – 7.93 (m, 2H), 7.80 (m, *J* = 7.8, 1.9 Hz, 1H), 7.65 – 7.51 (m, 6H), 7.46 – 7.36 (m, 3H), 5.02 (s, 2H); ^{13}C NMR (125 MHz, DMSO-d_6) δ 166.5, 152.5, 136.1, 134.4, 131.4, 130.6, 130.4, 129.2, 129.0, 128.3, 128.1, 128.1, 127.4, 126.2, 122.7, 46.1; LC-MS $[M + H]^+$: 335.1; HPLC purity at 254 nm, 100.0%.

4-(2-hydroxybenzyl)-2-(naphthalen-1-yl)-1,2,4-thiadiazolidine-3,5-dione (**TD1**). Obtained in 75% yield; white powder; ^{1}H NMR (400 MHz, DMSO-d_6) δ 9.78 (s, 1H), 8.10 (t, *J* = 7.2 Hz, 2H), 7.93 (d, *J* = 7.6 Hz, 1H), 7.80 (d, *J* = 7.3 Hz, 1H), 7.77 – 7.55 (m, 3H), 7.13 (d, *J* = 7.3 Hz, 2H), 6.85 (dd, *J* = 15.4, 7.6 Hz, 2H), 4.86 (s, 2H); ^{13}C NMR (125 MHz, $CDCl_3$) δ 166.7, 155.7, 153.7, 134.6, 132.5, 131.0, 130.9, 130.2, 130.2, 128.8, 127.9, 127.4, 127.2, 125.4, 122.0, 121.1, 120.8, 118.5, 42.2; LC-MS $[M + H]^+$: 351.1; HRMS $[M + H]^+$ (ESI - TOF) calcd for $C_{19}H_{14}N_2O_3S$ 351.0803, found 351.1332; HPLC purity at 254 nm, 100.0%.

4-(3-hydroxybenzyl)-2-(naphthalen-1-yl)-1,2,4-thiadiazolidine-3,5-dione (**TD2**). Obtained in 70% yield; white powder; ^{1}H NMR (400 MHz, DMSO-d_6) δ 9.54 (s, 1H), 8.10 (t, *J* = 8.2 Hz, 2H), 7.98 – 7.84 (m, 1H), 7.79 (d, *J* = 7.1 Hz, 1H), 7.74 – 7.51 (m, 3H), 7.19 (t, *J* = 8.0 Hz, 1H), 6.82 (d, *J* = 6.5 Hz, 2H), 6.73 (d, *J* = 8.8 Hz, 1H), 4.81 (s, 2H); ^{13}C NMR (125 MHz, $CDCl_3$) δ 165.7, 155.5, 152.0, 136.3, 134.1, 130.5, 130.0, 129.7, 129.6, 129.3, 128.3, 127.3, 127.0, 126.6, 125.0, 121.8, 121.1, 115.5, 115.1, 45.7; LC-MS $[M + H]^+$: 351.1; HRMS $[M + H]^+$ (ESI - TOF) calcd for $C_{19}H_{14}N_2O_3S$ 351.0803, found 351.0801; HPLC purity at 254 nm, 100.0%.

4-(4-hydroxybenzyl)-2-(naphthalen-1-yl)-1,2,4-thiadiazolidine-3,5-dione (**TD3**). Obtained in 78% yield; white powder; ^{1}H NMR (400 MHz, DMSO-d_6) δ 9.51 (s, 1H), 8.09 (dd, *J* = 10.0, 5.9 Hz, 2H), 7.85 (dd, *J* = 6.1, 3.5 Hz, 1H), 7.77 (d, *J* = 7.0 Hz, 1H), 7.69 – 7.57 (m, 3H), 7.23 (d, *J* = 8.5 Hz, 2H), 6.78 (d, *J* = 8.5 Hz, 2H), 4.77 (s, 2H); ^{13}C NMR (125 MHz, $CDCl_3$) δ 165.8, 155.3, 152.1, 134.1, 130.6, 130.0, 128.3, 127.2, 127.2, 126.9, 125.0, 121.8, 115.1, 45.4; LC-MS $[M + H]^+$: 351.1; HRMS $[M + H]^+$ (ESI - TOF)

calcd for $C_{19}H_{14}N_2O_3S$ 351.0803, found 351.0792; HPLC purity at 254 nm, 96.5%.

4-(4-fluorobenzyl)-2-(naphthalen-1-yl)-1,2,4-thiadiazolidine-3,5-dione (**TD4**).

Obtained in 26% yield; off-white powder; ^{1}H NMR (400 MHz, $CDCl_3$) δ 7.97 (d, *J* = 7.5 Hz, 2H), 7.78 (s, 1H), 7.71 – 7.48 (m, 6H), 7.09 (d, *J* = 7.9 Hz, 2H), 4.98 (d, *J* = 7.5 Hz, 2H). ^{13}C NMR (125 MHz, $CDCl_3$) δ 166.2, 163.8, 161.8, 152.4, 134.6, 131.1, 130.5, 128.8, 127.7, 127.4, 127.0, 125.4, 122.2, 115.8, 115.7, 45.7; LC-MS $[M + H]^+$: 353.1; HRMS $[M + H]^+$ (ESI - TOF) calcd for $C_{19}H_{13}FN_2O_2S$ 353.0760, found 353.0753; HPLC purity at 254 nm, 97.8%.

4-(4-chlorobenzyl)-2-(naphthalen-1-yl)-1,2,4-thiadiazolidine-3,5-dione (**TD5**).

Obtained in 67% yield; white powder; ^{1}H NMR (400 MHz, $CDCl_3$) δ 8.38 (d, *J* = 8.1 Hz, 1H), 7.80 (d, *J* = 8.2 Hz, 1H), 7.75 – 7.59 (m, 3H), 7.58 – 7.48 (m, 3H), 7.38 (d, *J* = 8.3 Hz, 2H), 4.96 (s, 2H);^{13}C NMR (125 MHz, $CDCl_3$) δ 165.9, 152.3, 134.6, 133.5, 131.8, 131.4, 130.7, 130.0, 129.1, 128.5, 128.2, 127.4, 125.8, 125.6, 122.7, 45.7; LC-MS $[M + H]^+$: 369.1; HRMS $[M + H]^+$ (ESI - TOF) calcd for $C_{19}H_{13}ClN_2O_2S$ 369.0465, found 369.0461; HPLC purity at 254 nm, 99.6%.

4-(3,4-dichlorobenzyl)-2-(naphthalen-1-yl)-1,2,4-thiadiazolidine-3,5-dione (**TD6**).

Obtained in 75% yield; white powder; ^{1}H NMR (400 MHz, DMSO-d_6) δ 8.30 (d, *J* = 8.3 Hz, 1H), 8.09 (d, *J* = 7.8 Hz, 1H), 7.85 (s, 2H), 7.83 – 7.75 (m, 2H), 7.73 – 7.62 (m, 3H), 7.43 (d, *J* = 8.2 Hz, 1H), 4.90 (s, 2H); ^{13}C NMR (125 MHz, DMSO-d_6) δ 166.7, 152.4, 137.2, 132.9, 131.8, 131.6, 131.4, 131.2, 131.1, 131.0, 130.5, 129.1, 129.1, 128.9, 128.7, 126.8, 125.0, 124.0, 45.1; LC-MS $[M + H]^+$: 403.0; HRMS $[M + H]^+$ (ESI - TOF)

calcd for $C_{19}H_{12}Cl_2N_2O_2S$ 403.0069, found 403.0075; HPLC purity at 254 nm, 99.6%.

4-(4-methylbenzyl)-2-(naphthalen-1-yl)-1,2,4-thiadiazolidine-3,5-dione (**TD7**). Obtained in 70% yield; white powder; ^{1}H NMR (400 MHz, $CDCl_3$) δ 8.41 – 8.34 (m, 1H), 7.85 – 7.81 (m, 1H), 7.72 – 7.66 (m, 2H), 7.64 (d, *J* = 7.9 Hz, 1H), 7.59 (s, 1H), 7.53 (d, *J* = 8.0 Hz, 1H), 7.46 (d, *J* = 8.0 Hz, 2H), 7.22 (d, *J* = 7.8 Hz, 2H), 4.97 (d, *J* = 3.3 Hz, 2H), 2.39 (s, 3H); ^{13}C NMR (125 MHz, $CDCl_3$) δ 165.9, 152.5, 138.4, 134.3, 132.2, 131.8, 131.5, 130.2, 129.5, 129.2, 128.4, 128.1, 127.4, 125.8, 125.5, 122.8, 46.3, 21.2; LC-MS $[M + H]^+$: 349.1; HRMS $[M + H]^+$ (ESI - TOF) calcd for $C_{20}H_{16}N_2O_2S$ 349.1011, found 349.1011; HPLC purity at 254 nm, 95.7%.

4-methyl-2-(naphthalen-1-yl)-1,2,4-thiadiazolidine-3,5-dione (**TD8**). Obtained in 56% yield; white powder; ^{1}H NMR (400 MHz, $CDCl_3$) δ 7.97 (t, *J* = 7.6 Hz, 2H), 7.87 (d, *J* = 8.1 Hz, 1H), 7.68 – 7.50 (m, 4H), 3.40 (s, 3H); ^{13}C NMR (125 MHz, DMSO-d_6) δ 166.0, 152.2, 134.2, 130.6, 130.1, 130.1, 128.3, 127.3, 127.0, 126.6, 125.1, 121.9, 28.5; LC-MS $[M + H]^+$: 259.1; HRMS $[M + H]^+$ (ESI - TOF) calcd for $C_{13}H_{10}N_2O_2S$ 259.0541, found 259.0532; HPLC purity at 254 nm, 99.0%.

4-ethyl-2-(naphthalen-1-yl)-1,2,4-thiadiazolidine-3,5-dione (**TD9**). Obtained in 47% yield; white powder; ^{1}H NMR (400 MHz, DMSO-d_6) δ 8.09 (dd, *J* = 10.5, 5.2 Hz, 2H), 7.95 – 7.88 (m, 1H), 7.78 (d, *J* = 7.3 Hz, 1H), 7.64 (dq, *J* = 15.1, 7.5 Hz, 3H), 3.76 (q, *J* = 7.1 Hz, 2H), 1.27 (t, *J* = 7.1 Hz, 3H); ^{13}C NMR (125 MHz, DMSO-d_6) δ 166.3, 152.4, 134.5, 131.6, 130.6, 130.5, 129.0, 128.4, 128.3, 128.1, 127.4, 126.3, 122.9, 38.2, 13.4; LC-MS $[M + H]^+$: 273.1; HRMS $[M + H]^+$ (ESI - TOF) calcd for $C_{14}H_{12}N_2O_2S$ 273.0698,

found 273.0696; HPLC purity at 254 nm, 98.0%.

4-butyl-2-(naphthalen-1-yl)-1,2,4-thiadiazolidine-3,5-dione (**TD10**). Obtained in 60% yield; white powder; ^{1}H NMR (400 MHz, DMSO-d_6) δ 8.09 (t, *J* = 7.2 Hz, 2H), 7.89 (d, *J* = 7.8 Hz, 1H), 7.77 (d, *J* = 7.3 Hz, 1H), 7.70 – 7.58 (m, 3H), 3.72 (t, *J* = 7.1 Hz, 2H), 1.77 – 1.55 (m, 2H), 1.38 (dd, *J* = 14.8, 7.4 Hz, 2H), 0.94 (t, *J* = 7.3 Hz, 3H); ^{13}C NMR (125 MHz, DMSO-d_6) δ 166.5, 152.6, 134.5, 131.6, 130.6, 130.5, 129.1, 128.3, 128.1, 127.4, 126.3, 122.9, 42.7, 29.8, 19.9, 14.0; LC-MS $[M + H]^+$: 301.2; HRMS $[M + H]^+$ (ESI - TOF) calcd for $C_{16}H_{16}N_2O_2S$ 301.1011, found 301.0998; HPLC purity at 254 nm, 97.9%.

2-(naphthalen-1-yl)-4-phenethyl-1,2,4-thiadiazolidine-3,5-dione (**TD11**). Obtained in 80% yield; white powder; ^{1}H NMR (400 MHz, $CDCl_3$) δ 7.95 (m, *J* = 6.3, 5.5, 2.3 Hz, 2H), 7.67 – 7.51 (m, 5H), 7.44 – 7.30 (m, 5H), 4.15 – 4.08 (m, 2H), 3.22 – 3.11 (m, 2H); ^{13}C NMR (125 MHz, DMSO-d_6) δ 166.3, 152.2, 138.2, 134.4, 131.5, 130.5, 130.5, 129.4, 129.0, 128.2, 128.1, 127.4, 127.1, 126.3, 122.8, 44.0, 33.1; LC-MS $[M + H]^+$: 349.1; HRMS $[M + H]^+$ (ESI - TOF) calcd for $C_{20}H_{16}N_2O_2S$ 349.1011, found 349.1016; HPLC purity at 254 nm, 99.9%.

2-benzyl-4-methyl-1,2,4-thiadiazolidine-3,5-dione (**TD12**). Obtained in 52% yield; white powder; ^{1}H NMR (400 MHz, DMSO-d_6) δ 7.37 (dt, *J* = 15.3, 7.2 Hz, 5H), 4.80 (s, 2H), 3.08 (s, 3H); ^{13}C NMR (125 MHz, DMSO-d_6) δ 165.9, 153.0, 135.6, 128.8, 128.2, 128.1, 47.5, 28.4; LC-MS $[M + H]^+$: 223.1; HRMS $[M + H]^+$ (ESI - TOF) calcd for $C_{10}H_{10}N_2O_2S$ 223.0541, found 223.0534; HPLC purity at 254 nm, 99.2%.

2-benzyl-4-butyl-1,2,4-thiadiazolidine-3,5-dione (**TD13**). Obtained in 55% yield; white

powder; ^{1}H NMR (400 MHz, $CDCl_3$) δ 7.39 (dd, *J* = 13.0, 7.5 Hz, 3H), 7.32 (d, *J* = 7.7 Hz, 2H), 4.80 (s, 2H), 3.73 (t, *J* = 7.4 Hz, 2H), 1.75 – 1.65 (m, 2H), 1.39 (dd, *J* = 15.1, 7.5 Hz, 2H), 0.98 (t, *J* = 7.3 Hz, 3H); ^{13}C NMR (125 MHz, $CDCl_3$) δ 166.0, 153.4, 134.6, 129.1, 128.8, 128.5, 48.7, 42.6, 29.9, 19.9, 13.6; LC-MS $[M + H]^+$: 265.1; HRMS $[M + H]^+$ (ESI - TOF) calcd for $C_{13}H_{16}N_2O_2S$ 265.1011, found 265.1031; HPLC purity at 254 nm, 98.0%.

2-benzyl-4-(2-chloroethyl)-1,2,4-thiadiazolidine-3,5-dione (**TD14**). Obtained in 66% yield; white powder; ^{1}H NMR (400 MHz, $CDCl_3$) δ 7.45 – 7.37 (m, 3H), 7.36 – 7.30 (m, 2H), 4.81 (s, 2H), 4.07 (t, *J* = 6.3 Hz, 2H), 3.80 (t, *J* = 6.3 Hz, 2H); ^{13}C NMR (125 MHz, $CDCl_3$) δ 165.9, 152.7, 134.3, 129.1, 129.0, 128.7, 128.7, 128.5, 127.5, 127.5, 48.8, 43.6, 39.9; LC-MS $[M + H]^+$: 271.1; HRMS $[M + H]^+$ (ESI - TOF) calcd for $C_{11}H_{11}ClN_2O_2S$ 271.0308, found 271.0311; HPLC purity at 254 nm, 99.4%.

2-benzyl-4-isopropyl-1,2,4-thiadiazolidine-3,5-dione (**TD15**). Obtained in 25% total yield; white powder; ^{1}H NMR (400 MHz, $CDCl_3$) δ 7.44 – 7.36 (m, 3H), 7.35 – 7.30 (m, 2H), 4.78 (s, 2H), 4.59 (dt, *J* = 13.9, 6.9 Hz, 1H), 1.52 (s, 3H), 1.50 (s, 3H); ^{13}C NMR (125 MHz, $CDCl_3$) δ 165.8, 153.1, 134.7, 129.0, 128.8, 128.5, 48.7, 48.2, 19.3; LC-MS $[M + H]^+$: 251.2; HRMS $[M + H]^+$ (ESI - TOF) calcd for $C_{12}H_{14}N_2O_2S$ 251.0854, found 251.0860; HPLC purity at 254 nm, 96.9%.

2-benzyl-4-(3-fluorophenyl)-1,2,4-thiadiazolidine-3,5-dione (**TD16**). Obtained in 28% yield; white powder; ^{1}H NMR (400 MHz, $CDCl_3$) δ 7.53 (d, *J* = 7.5 Hz, 2H), 7.48 – 7.32 (m, 5H), 7.32 – 7.21 (m, 1H), 7.00 (t, *J* = 8.2 Hz, 1H), 4.94 (s, 2H); ^{13}C NMR (125 MHz, $CDCl_3$) δ 164.5, 163.8, 161.9, 150.8, 137.2, 134.8, 130.7, 130.7, 129.1, 128.8, 128.5,

118.0, 118.0, 113.8, 113.6, 110.8, 110.6, 46.3; LC-MS $[M + H]^+$: 303.1; HRMS $[M + H]^+$ (ESI - TOF) calcd for $C_{15}H_{11}FN_2O_2S$ 303.0604, found 303.0600; HPLC purity at 254 nm, 96.4%.

2,4-dibenzyl-1,2,4-thiadiazolidine-3,5-dione (**TD17**). Obtained in 23% yield; white powder; ^1H NMR (400 MHz, $CDCl_3$) δ 7.49 (dd, *J* = 7.8, 1.5 Hz, 2H), 7.45 – 7.35 (m, 6H), 7.34 – 7.29 (m, 2H), 4.88 (s, 2H), 4.80 (s, 2H); ^{13}C NMR (125 MHz, $CDCl_3$) δ 165.9, 153.1, 135.2, 134.5, 128.9, 128.5, 128.3, 48.8, 46.0; LC-MS $[M + H]^+$: 299.2; HRMS $[M + H]^+$ (ESI - TOF) calcd for $C_{16}H_{14}N_2O_2S$ 299.0854, found 299.0846; HPLC purity at 254 nm, 96.3%.

2-benzyl-4-(4-methylbenzyl)-1,2,4-thiadiazolidine-3,5-dione (**TD18**). Obtained in 55% yield; white powder; ^1H NMR (400 MHz, DMSO-d_6) δ 7.43 – 7.27 (m, 5H), 7.19 (dd, *J* = 18.3, 7.8 Hz, 4H), 4.82 (s, 2H), 4.73 (s, 2H), 2.28 (s, 3H); ^{13}C NMR (125 MHz, DMSO-d_6) δ 165.7, 152.8, 137.1, 135.5, 132.8, 129.2, 128.8, 128.3, 128.1, 127.7, 47.6, 45.0, 20.7; LC-MS $[M + H]^+$: 313.1; HRMS $[M + H]^+$ (ESI - TOF) calcd for $C_{17}H_{16}N_2O_2S$ 313.1011, found 313.1005; HPLC purity at 254 nm, 99.1%.

2-benzyl-4-(2-chlorobenzyl)-1,2,4-thiadiazolidine-3,5-dione (**TD19**). Obtained in 50% yield; white powder; ^1H NMR (400 MHz, DMSO-d_6) δ 7.51 (dd, *J* = 8.5, 4.6 Hz, 1H), 7.39 (dt, *J* = 12.2, 8.2 Hz, 7H), 7.24 – 7.16 (m, 1H), 4.87 (s, 2H), 4.85 (s, 2H); ^{13}C NMR (125 MHz, DMSO-d_6) δ 165.8, 152.6, 135.5, 132.6, 131.8, 129.6, 129.4, 128.8, 128.3, 128.3, 128.1, 127.5, 47.7, 43.0; LC-MS $[M + H]^+$: 333.1; HRMS $[M + H]^+$ (ESI - TOF) calcd for $C_{16}H_{13}ClN_2O_2S$ 333.0465, found 333.0450; HPLC purity at 254 nm, 97.3%.

2-benzyl-4-(3,4-dichlorobenzyl)-1,2,4-thiadiazolidine-3,5-dione (**TD20**). Obtained in 67% yield; white powder; ^{1}H NMR (400 MHz, DMSO-d_6) δ 7.64 (d, *J* = 8.3 Hz, 1H), 7.59 (s, 1H), 7.44 – 7.23 (m, 6H), 4.82 (s, 2H), 4.79 (s, 2H); ^{13}C NMR (125 MHz, DMSO-d_6) δ 165.9, 152.6, 136.8, 135.5, 131.2, 130.9, 130.6, 129.8, 128.8, 128.3, 128.1, 128.0, 47.7, 44.1; LC-MS [M + H]$^+$: 367.0; HRMS [M + H]$^+$ (ESI - TOF) calcd for $C_{16}H_{12}Cl_2N_2O_2S$ 367.0075, found 367.0077; HPLC purity at 254 nm, 99.6%.

4-(4-chlorobenzyl)-2-ethyl-1,2,4-thiadiazolidine-3,5-dione (**TD21**). Obtained in 61% yield; white powder; ^{1}H NMR (400 MHz, $CDCl_3$) δ 7.41 (d, *J* = 8.4 Hz, 2H), 7.35 – 7.30 (m, 2H), 4.80 (s, 2H), 3.71 (q, *J* = 7.2 Hz, 2H), 1.29 (t, *J* = 7.2 Hz, 3H); ^{13}C NMR (125 MHz, $CDCl_3$) δ 165.9, 152.6, 134.3, 133.7, 130.4, 128.9, 45.2, 40.1, 13.9; LC-MS [M + H]$^+$: 271.1; HRMS [M + H]$^+$ (ESI - TOF) calcd for $C_{11}H_{11}ClN_2O_2S$ 271.0308, found 271.0304; HPLC purity at 254 nm, 99.8%.

2-ethyl-4-(4-methylbenzyl)-1,2,4-thiadiazolidine-3,5-dione (**TD22**). Obtained in 72% yield; white powder; ^{1}H NMR (400 MHz, $CDCl_3$) δ 7.37 (d, *J* = 7.9 Hz, 2H), 7.17 (d, *J* = 7.8 Hz, 2H), 4.80 (s, 2H), 3.70 (q, *J* = 7.2 Hz, 2H), 2.35 (s, 3H), 1.28 (t, *J* = 7.2 Hz, 3H); ^{13}C NMR (125 MHz, $CDCl_3$) δ 166.0, 152.8, 138.1, 132.4, 129.4, 128.9, 45.7, 40.0, 21.2, 13.9; LC-MS [M + H]$^+$: 251.1; HRMS [M + H]$^+$ (ESI - TOF) calcd for $C_{12}H_{14}N_2O_2S$ 251.0854, found 251.0856; HPLC purity at 254 nm, 98.6%.

2-ethyl-4-phenethyl-1,2,4-thiadiazolidine-3,5-dione (**TD23**). Obtained in 49% yield; colorless oil; ^{1}H NMR (400 MHz, $CDCl_3$) δ 7.36 – 7.29 (m, 2H), 7.28 – 7.22 (m, 3H), 3.99 – 3.88 (m, 2H), 3.73 – 3.66 (m, 2H), 3.00 (dd, *J* = 8.7, 6.8 Hz, 2H), 1.30 – 1.21 (m,

3H); ^{13}C NMR (125 MHz, $CDCl_3$) δ 165.9, 152.7, 137.4, 128.9, 128.6, 126.8, 43.7, 40.0, 33.8, 13.8; LC-MS $[M + H]^+$: 251.1; HRMS $[M + H]^+$ (ESI - TOF) calcd for $C_{12}H_{14}N_2O_2S$ 251.0854, found 251.0857; HPLC purity at 254 nm, 95.4%.

2,4-dibutyl-1,2,4-thiadiazolidine-3,5-dione (**TD24**). Obtained in 57% yield; white powder; ^{1}H NMR (400 MHz, $CDCl_3$) δ 3.66 (dtd, *J* = 18.5, 7.3, 1.1 Hz, 4H), 1.71 – 1.57 (m, 4H), 1.44 – 1.30 (m, 4H), 0.95 (tdd, *J* = 7.3, 4.4, 1.1 Hz, 6H); ^{13}C NMR (125 MHz, $CDCl_3$) δ 166.1, 153.2, 44.6, 42.5, 30.7, 29.8, 30.7, 29.8, 19.9, 19.6, 13.6, 13.5; LC-MS $[M + H]^+$: 231.1; HRMS $[M + H]^+$ (ESI - TOF) calcd for $C_{10}H_{18}N_2O_2S$ 231.1167, found 231.1162; HPLC purity at 254 nm, 99.0%.

4-cyclohexyl-2-cyclopentyl-1,2,4-thiadiazolidine-3,5-dione (**TD25**). Obtained in 43% yield; colorless oil; ^{1}H NMR (400 MHz, $CDCl_3$) δ 4.79 (dd, *J* = 15.0, 7.6 Hz, 1H), 4.14 (tt, *J* = 12.3, 3.9 Hz, 1H), 3.50 – 3.41 (m, 1H), 2.23 (qd, *J* = 12.4, 3.3 Hz, 2H), 2.13 – 2.01 (m, 2H), 1.86 (d, *J* = 13.7 Hz, 2H), 1.78 (m, 4H), 1.71 (m, 2H), 1.58 (m, 2H), 1.43 – 1.17 (m, 3H); ^{13}C NMR (125 MHz, $CDCl_3$) δ 167.6, 154.2, 57.3, 57.1, 32.5, 30.3, 27.3, 26.4, 25.4; LC-MS $[M + H]^+$: 269.1; HRMS $[M + H]^+$ (ESI - TOF) calcd for $C_{13}H_{20}N_2O_2S$ 269.1324, found 269.1322; HPLC purity at 254 nm, 96.4%.

4-benzyl-2-phenethyl-1,2,4-thiadiazolidine-3,5-dione (**TD26**). Obtained in 21% yield; white powder; ^{1}H NMR (400 MHz, $CDCl_3$) δ 7.48 – 7.14 (m, 10H), 4.81 (s, 2H), 3.90 (t, *J* = 7.2 Hz, 2H), 2.96 (t, *J* = 7.2 Hz, 2H); ^{13}C NMR (125 MHz, $CDCl_3$) δ 165.9, 152.9, 136.9, 135.2, 128.8, 128.2, 127.1, 46.2, 45.9, 34.9; LC-MS $[M + H]^+$: 313.1; HRMS $[M + H]^+$ (ESI - TOF) calcd for $C_{17}H_{16}N_2O_2S$ 313.1011, found 313.1010; HPLC purity at 254

nm, 99.4%.

4-cyclohexyl-2-phenethyl-1,2,4-thiadiazolidine-3,5-dione (**TD27**). Obtained in 28% yield; white powder; ^{1}H NMR (400 MHz, $CDCl_3$) δ 7.34 (t, *J* = 7.1 Hz, 2H), 7.28 (q, *J* = 2.9 Hz, 1H), 7.24 (dd, *J* = 7.7, 6.3 Hz, 2H), 4.18 – 4.03 (m, 1H), 3.87 (t, *J* = 7.3 Hz, 2H), 2.96 (t, *J* = 7.3 Hz, 2H), 2.20 (qd, *J* = 12.4, 3.2 Hz, 2H), 1.86 (d, *J* = 13.5 Hz, 2H), 1.68 (t, *J* = 11.6 Hz, 3H), 1.41 – 1.16 (m, 3H); ^{13}C NMR (125 MHz, $CDCl_3$) δ 166.0, 153.1, 137.0, 128.8, 127.0, 55.9, 46.1, 34.8, 28.8, 25.9, 24.9; LC-MS $[M + H]^+$: 305.3; HRMS $[M + H]^+$ (ESI - TOF) calcd for $C_{16}H_{20}N_2O_2S$ 305.1324, found 305.1317; HPLC purity at 254 nm, 99.0%.

4-isopropyl-2-phenethyl-1,2,4-thiadiazolidine-3,5-dione (**TD28**). Obtained in 26% yield; white powder; ^{1}H NMR (400 MHz, $CDCl_3$) δ 7.37 – 7.30 (m, 2H), 7.30 – 7.26 (m, 1H), 7.24 (dd, *J* = 6.9, 5.5 Hz, 2H), 4.51 (dt, *J* = 13.9, 6.9 Hz, 1H), 3.87 (t, *J* = 7.3 Hz, 2H), 2.96 (t, *J* = 7.2 Hz, 2H), 1.46 (s, 3H), 1.44 (s, 3H); ^{13}C NMR (125 MHz, $CDCl_3$) δ 165.8, 153.0, 137.0, 128.8, 127.0, 48.1, 46.1, 34.9, 19.2; LC-MS $[M + H]^+$: 265.2; HRMS $[M + H]^+$ (ESI - TOF) calcd for $C_{13}H_{16}N_2O_2S$ 265.1011, found 265.1006; HPLC purity at 254 nm, 99.8%.

2-(benzo[d][1,3]dioxol-4-yl)-4-benzyl-1,2,4-thiadiazolidine-3,5-dione (**TD29**). Obtained in 48% yield; white powder; ^{1}H NMR (400 MHz, $CDCl_3$) δ 7.52 (dd, *J* = 7.7, 1.7 Hz, 2H), 7.42 – 7.33 (m, 3H), 6.98 – 6.82 (m, 3H), 6.07 (s, 2H), 4.94 (s, 2H); ^{13}C NMR (125 MHz, $CDCl_3$) δ 165.8, 151.3, 149.2, 143.0, 135.0, 129.1, 128.8, 128.4, 122.3, 119.9, 117.2, 108.9, 102.1, 46.3; LC-MS $[M + H]^+$: 329.1; HRMS $[M + H]^+$ (ESI - TOF) calcd for $C_{16}H_{12}N_2O_4S$ 329.0596, found 329.0582; HPLC purity at 254 nm, 97.3%.

4-benzyl-2-(2,3-dihydro-1H-inden-4-yl)-1,2,4-thiadiazolidine-3,5-dione (**TD30**)**.** Obtained in 24% yield; off-white powder; ^{1}H NMR (400 MHz, $CDCl_3$) δ 7.53 (dd, *J* = 7.7, 1.5 Hz, 2H), 7.43 – 7.32 (m, 3H), 7.27 (s, 1H), 7.22 (t, *J* = 7.5 Hz, 1H), 7.16 (d, *J* = 7.5 Hz, 1H), 4.94 (s, 2H), 2.99 (t, *J* = 7.5 Hz, 2H), 2.90 (t, *J* = 7.4 Hz, 2H), 2.22 – 2.06 (m, 2H). ^{13}C NMR (125 MHz, $CDCl_3$) δ 166.1, 151.3, 147.3, 142.43, 135.23, 131.0, 129.0, 128.8, 128.38, 127.6, 125.3, 124.7, 46.2, 33.1, 31.1, 25.0; LC-MS $[M + H]^+$: 325.2; HRMS $[M + H]^+$ (ESI - TOF) calcd for $C_{18}H_{16}N_2O_2S$ 325.1011, found 325.1000; HPLC purity at 254 nm, 99.3%.

4-benzyl-2-(5,6,7,8-tetrahydronaphthalen-1-yl)-1,2,4-thiadiazolidine-3,5-dione (**TD31**)**.** Obtained in 21% yield; off-white powder; ^{1}H NMR (400 MHz, $CDCl_3$) δ 7.52 (dd, *J* = 7.7, 1.6 Hz, 2H), 7.38 (d, *J* = 7.7 Hz, 3H), 7.17 (t, *J* = 4.7 Hz, 3H), 4.94 (s, 2H), 2.82 (s, 2H), 2.64 (s, 2H), 1.81 (d, *J* = 2.8 Hz, 4H). ^{13}C NMR (125 MHz, $CDCl_3$) δ 166.2, 151.7, 139.7, 136.7, 135.3, 133.0, 130.9, 129.0, 128.8, 128.3, 126.3, 126.1, 46.2, 41.0, 29.5, 24.8, 22.4; LC-MS $[M + H]^+$: 339.1; HRMS $[M + H]^+$ (ESI - TOF) calcd for $C_{19}H_{18}N_2O_2S$ 339.1167, found 339.1151; HPLC purity at 254 nm, 100.0%.

General synthesis of compounds TD32-**TD40.** Triphosgene (1.6 mmol) was added to a solution of 3,5-dimethylisoxazol-4-amine (**4**, 2.0 mmol) in anhydrous THF, and the mixture was stirred at 50 °C for 1 hr. The solution was concentrated, and yellow oil **2'** was mixed with isothiocyanate (**1**, 2.0 mmol) in anhydrous THF. Sulfuryl chloride (2.0 mmol) was added dropwise at 0 °C, and the mixture was warmed to rt and then stirred for 4-10 hr. The mixture was concentrated under vacuum and purified by RP-C18 column chromatography to give the target products.

4-benzyl-2-(3,5-dimethylisoxazol-4-yl)-1,2,4-thiadiazolidine-3,5-dione (**TD32**). Obtained in 76% yield; white powder; ^{1}H NMR (400 MHz, DMSO-d_6) δ 7.59 – 7.13 (m, 5H), 4.83 (s, 2H), 2.39 (s, 3H), 2.16 (s, 3H); ^{13}C NMR (125 MHz, DMSO-d_6) δ 168.4, 166.3, 158.5, 152.2, 135.8, 129.3, 129.2, 129.1, 129.0, 128.4, 127.9, 112.3, 46.0, 11.1, 9.6; LC-MS $[M + H]^+$: 304.0; HRMS $[M + H]^+$ (ESI - TOF) calcd for $C_{14}H_{13}N_3O_3S$ 304.0756, found 304.0754; HPLC purity at 254 nm, 99.4%.

2-(3,5-dimethylisoxazol-4-yl)-4-ethyl-1,2,4-thiadiazolidine-3,5-dione (**TD33**). Obtained in 41% yield; colorless oil; ^{1}H NMR (400 MHz, $CDCl_3$) δ 3.86 (q, *J* = 7.2 Hz, 2H), 2.42 (s, 3H), 2.25 (s, 3H), 1.35 (t, *J* = 7.2 Hz, 3H); ^{13}C NMR (125 MHz, $CDCl_3$) δ 167.9, 165.3, 158.0, 151.9, 112.1, 38.5, 13.1, 11.3, 9.7; LC-MS $[M + H]^+$: 242.1; HRMS $[M + H]^+$ (ESI - TOF) calcd for $C_9H_{11}N_3O_3S$ 242.0599, found 242.0587; HPLC purity at 254 nm, 98.2%.

4-butyl-2-(3,5-dimethylisoxazol-4-yl)-1,2,4-thiadiazolidine-3,5-dione (**TD34**). Obtained in 60% yield; colorless oil; ^{1}H NMR (400 MHz, $CDCl_3$) δ 3.85 – 3.74 (m, 2H), 2.42 (s, 3H), 2.26 (s, 3H), 1.78 – 1.69 (m, 2H), 1.42 (dd, *J* = 15.2, 7.5 Hz, 2H), 1.00 (t, *J* = 7.4 Hz, 3H); ^{13}C NMR (125 MHz, $CDCl_3$) δ 167.8, 165.4, 157.9, 152.0, 112.1, 43.1, 29.7, 19.8, 13.5, 11.2, 9.7; LC-MS $[M + H]^+$: 270.1; HRMS $[M + H]^+$ (ESI - TOF) calcd for $C_{11}H_{15}N_3O_3S$ 270.0912, found 270.0902; HPLC purity at 254 nm, 98.0%.

2-(3,5-dimethylisoxazol-4-yl)-4-isopropyl-1,2,4-thiadiazolidine-3,5-dione (**TD35**). Obtained in 53% yield; colorless oil; ^{1}H NMR (400 MHz, $CDCl_3$) δ 4.63 (dt, *J* = 13.8, 6.9 Hz, 1H), 2.41 (s, 3H), 2.24 (s, 3H), 1.55 (d, *J* = 6.9 Hz, 6H); ^{13}C NMR (125 MHz, $CDCl_3$) δ 167.7, 165.2, 158.0, 151.9, 112.3, 49.0, 19.2, 11.3, 9.7; LC-MS $[M + H]^+$: 256.1; HRMS

$[M + H]^+$ (ESI - TOF) calcd for $C_{10}H_{13}N_3O_3S$ 256.0756, found 256.0746; HPLC purity at 254 nm, 98.7%.

2-(3,5-dimethylisoxazol-4-yl)-4-(4-methylbenzyl)-1,2,4-thiadiazolidine-3,5-dione (**TD36**). Obtained in 81% yield; white powder; ^1H NMR (400 MHz, $CDCl_3$) δ 7.39 (d, *J* = 8.0 Hz, 2H), 7.20 (d, *J* = 7.8 Hz, 2H), 4.89 (s, 2H), 2.40 (s, 3H), 2.37 (s, 3H), 2.23 (s, 3H); ^{13}C NMR (125 MHz, $CDCl_3$) δ 167.8, 165.2, 157.9, 151.9, 138.4, 131.8, 129.5, 129.0, 112.1, 46.3, 21.2, 11.3, 9.7; LC-MS $[M + H]^+$: 318.1; HRMS $[M + H]^+$ (ESI - TOF) calcd for $C_{15}H_{15}N_3O_3S$ 318.0912, found 318.0908; HPLC purity at 254 nm, 97.7%.

2-(3,5-dimethylisoxazol-4-yl)-4-(4-methoxybenzyl)-1,2,4-thiadiazolidine-3,5-dione (**TD37**). Obtained in 83% yield; white powder; ^1H NMR (400 MHz, $CDCl_3$) δ 7.45 (d, *J* = 8.6 Hz, 2H), 6.90 (d, *J* = 8.7 Hz, 2H), 4.87 (s, 2H), 3.83 (s, 3H), 2.39 (s, 3H), 2.22 (s, 3H); ^{13}C NMR (125 MHz, $CDCl_3$) δ 167.8, 165.3, 159.7, 157.9, 151.9, 130.6, 126.9, 114.1, 112.0, 55.2, 46.1, 11.3, 9.7; LC-MS $[M + H]^+$: 334.1; HRMS $[M + H]^+$ (ESI - TOF) calcd for $C_{15}H_{15}N_3O_4S$ 334.0862, found 334.0851; HPLC purity at 254 nm, 98.7%.

4-(3,4-dichlorobenzyl)-2-(3,5-dimethylisoxazol-4-yl)-1,2,4-thiadiazolidine-3,5-dione (**TD38**). Obtained in 71% yield; white powder; ^1H NMR (400 MHz, $CDCl_3$) δ 7.60 (d, *J* = 2.0 Hz, 1H), 7.47 (d, *J* = 8.2 Hz, 1H), 7.34 (dd, *J* = 8.2, 2.0 Hz, 1H), 4.87 (s, 2H), 2.41 (s, 3H), 2.24 (s, 3H); ^{13}C NMR (125 MHz, $CDCl_3$) δ 167.9, 165.1, 157.8, 151.6, 134.6, 133.0, 133.0, 131.0, 130.9, 128.4, 45.3, 11.3, 9.8; LC-MS $[M + H]^+$: 372.0; HRMS $[M + H]^+$ (ESI - TOF) calcd for $C_{14}H_{11}Cl_2N_3O_3S$ 371.9976, found 371.9979; HPLC purity at 254 nm, 99.7%.

4-(2-chlorobenzyl)-2-(3,5-dimethylisoxazol-4-yl)-1,2,4-thiadiazolidine-3,5-dione **(TD39).** Obtained in 67% yield; white powder; ^{1}H NMR (400 MHz, $CDCl_3$) δ 7.47 – 7.40 (m, 1H), 7.31 (t, *J* = 3.4 Hz, 3H), 5.09 (s, 2H), 2.43 (s, 3H), 2.27 (s, 3H); ^{13}C NMR (125 MHz, $CDCl_3$) δ 168.0, 165.0, 157.9, 151.7, 133.3, 131.8, 130.0, 129.6, 129.1, 127.1, 112.0, 44.3, 11.3, 9.7; LC-MS $[M + H]^+$: 338.0; HRMS $[M + H]^+$ (ESI - TOF) calcd for $C_{14}H_{12}ClN_3O_3S$ 338.0366, found 338.0354; HPLC purity at 254 nm, 99.3%.

4-(4-chlorobenzyl)-2-(3,5-dimethylisoxazol-4-yl)-1,2,4-thiadiazolidine-3,5-dione **(TD40).** Obtained in 69% yield; white powder; ^{1}H NMR (400 MHz, $CDCl_3$) δ 7.49 (dd, *J* = 8.4, 5.4 Hz, 2H), 7.07 (t, *J* = 8.6 Hz, 2H), 4.89 (s, 2H), 2.40 (s, 3H), 2.22 (s, 3H); ^{13}C NMR (125 MHz, $CDCl_3$) δ 167.8, 165.2, 157.9, 151.8, 131.1, 131.0, 130.6, 115.9, 115.7, 112.0, 45.8, 11.3, 9.7; LC-MS $[M + H]^+$: 338.0;HRMS $[M + H]^+$ (ESI - TOF) calcd for $C_{14}H_{12}ClN_3O_3S$ 338.0366, found 338.0360; HPLC purity at 254 nm, 97.8%.

Protein expression and purification. This was performed following a published procedure.[38] The $srtA_{\Delta N24}$ or $srtA_{\Delta N59}$ gene was cloned into the pET28a vector, encoding an N-terminal His-tagged protein. The *Escherichia coli* BL21 (DE3) strain was transformed with recombinant plasmids and grown in a lysogeny broth medium containing 30 μg/mL kanamycin at 37 °C. When A_{600} reached 0.6, isopropyl β-D-thiogalactopyranose at a final concentration of 1 mM was added to induce SrtA expression, and growth continued for an additional 4 hr at 30 °C. The cells were collected by centrifugation and resuspended in 30 mL of Ni-NTA buffer A (50 mM Tris-HCl (pH 7.5), 200 mM NaCl, 40 mM imidazole, and 1 mM DTT) with phenylmethanesulfonyl fluoride as a protease inhibitor. The samples were then

purified by Ni-NTA (GE Healthcare) with a gradient washing using buffer B (50 mM Tris-HCl (pH 7.5), 200 mM NaCl, 300 mM imidazole, and 1 mM DTT). The fractions containing the targets were further purified by Superdex 75 gel-filtration chromatography (GE Healthcare) with desalting buffer (50 mM Tris-HCl (pH 7.5), 200 mM NaCl, and 1 mM DTT). The fractions were collected, concentrated, and estimated by 12% (w/v) SDS-PAGE analysis.

HTS for SrtA inhibitors. Stock concentrations of all the compounds were prepared in DMSO at a concentration of 10 mM. Before the screening, the compounds were added to a reaction buffer (50 mM Tris-HCl, 150 mM NaCl, 5 mM $CaCl_2$, and pH 7.5) containing 1 μM recombinant $SrtA_{\Delta N24}$ to a final concentration of 100 μM and then incubated at rt for 20 min. The peptide substrate (Abz-LPATG-Dnp) at a concentration of 10 μM was subsequently added to start the transpeptidation. The fluorescence was measured every 1 min for 20 min using Flex Station 3 (Molecular Devices) with the excitation and emission wavelengths set at 309 and 420 nm, respectively, to monitor the change in intensity. The initial velocities, V_0 and V_i, were obtained with and without inhibitor, respectively. The percent inhibition was calculated according to the following equation: inhibition ratio (%) = $(1 - V_i / V_0) \times 100\%$. Three technical replicates were performed on each compound.

IC_{50} determination. Compounds with inhibition ratios (%) against $SrtA_{\Delta N24}$ >50% were selected for IC_{50} determination. $SrtA_{\Delta N24}$ at 1 μM was incubated with the inhibitors at several concentrations (ranging from 0.2 μM to 100 μM) for 20 min at rt, and then 10 μM peptide substrate was added to the reaction buffer. The IC_{50} values were

determined using sigmoidal dose-response by GraphPad Prism software. Three technical replicates were taken for each data point, and the data are reported as the mean ± SEM. Three independent experiments were conducted on each compound.

Inhibition of SrtA transpeptidation on a protein substrate. The test compounds (1-25 μM) were added to 50 μL of reaction buffer (50 mM Tris-HCl, 150 mM NaCl, 5 mM $CaCl_2$, and pH 7.5) containing 100 μg $SrtA_{\Delta N24}$ and incubated at rt for 20 min. Then, 150 μg of $IsdA_{64–323}$ and 3 mM Gly_3 were added to the reaction. After incubation at 37 °C for 1.5 hr, the reactions were quenched with 12.5 μL 5 × SDS loading buffer. The samples were subjected to 12% (w/v) Tris-glycine SDS-PAGE analysis and photographed using Tanon 2500 Gel Image System with setting exposure time of 130 ms. The intensities of the $IsdA_{64-323}$ bands were analyzed in Image J. The IC_{50} values were calculated by GraphPad Prism software using sigmoidal dose-response. Three independent experiments were performed on each compound.

Bacterial growth assay. Overnight cultures of *S. aureus* were diluted 1:1000 with fresh tryptic soy broth (TSB). The diluted cultures were further cultured until A_{600} reached 0.6-0.8 and diluted again 1:400 with TSB. Two hundred microliter aliquots were added to 96-well microtiter plates (Cell Biolabs) with different concentrations of the test compounds. The A_{600} value of each well was measured every 1 hr for 24 hr using Flex Station 3 (Molecular Devices). The growth curve was drawn using GraphPad drawing, and each data point was measured in three technical replicates. Three independent experiments were performed on each compound.

Determination of solubility. A solution of **TD** or **TD32** in DMSO was prepared, and the standard curve was obtained by LC-MS for **TD** or HPLC for **TD32**. One milliliter of PBS and 10 μL of 100 mg/mL **TD** or **TD32** in DMSO were added to a colorless transparent glass bottle with a magnetic bar and stirred at 37 °C for 4 hr. The supernatant was collected and centrifuge, and the concentration was detected by LC-MS for **TD** or HPLC for **TD32**.

Circular dichroism. Compounds **TD** and **TD32** were dissolved in methanol to the indicated concentrations and then incubated with 10 μM $SrtA_{\Delta N24}$. Subsequently, the circular dichroism spectrum of each mixture was obtained on a J-810 Spectropolarimeter. Two independent experiments were performed on each compound.

Mass spectrometry analysis. $SrtA_{\Delta N24}$ was preincubated with or without a 10-fold excess of the test compounds for 12 hr. The protein was diluted with 50% acetonitrile and 0.2% formic acid and was injected onto a C8 column (Zorbax, 4.6 mm × 250 mm, Agilent). The sample was eluted with a 10-90% acetonitrile gradient over 11 min. The flow rate was 0.3 mL/min, and the data were acquired using an ESI-TOF mass spectrometer. The conditions included a capillary voltage of 5500 V, a drying gas flow rate of 13 L min^{-1}, a drying gas temperature of 300 °C, a nebulizer gas flow rate of 60 L min^{-1}, and a fragmentator voltage of 250 V.

Nuclear magnetic resonance titration. Phosphate buffer (20 mM sodium phosphate (pH 7.4) and 100 mM NaCl) in the presence of 2% DMSO was used for NMR titration.

All NMR spectra were acquired on a Bruker Avance III-600 MHz spectrometer equipped with a cryogenically cooled probe (Bruker Biospin, Germany) at 25 °C. Experimental samples contained 200 μM **TD32** and $SrtA_{\Delta N59}$ protein at 0 μM, 5 μM, 10 μM, 20 μM and 40 μM. Two independent experiments were performed.

AutoDock docking. The docking between the **TD** inhibitors and $SrtA_{\Delta N59}$ (PDB ID: 2KID) was conducted using AutoDock 4.2. The three-dimensional (3D) structure of the ligands was built and optimized by ChemBio 3D. The rotatable bonds in the ligands were defined using AutoTors, which also united the nonpolar hydrogens and partial atomic charges to the bonded carbon atoms. The ligand and SrtA structures were prepared with Gasteiger-Marsili charges in PDBQT files. The interaction grids were calculated for each receptor using the AutoGrid4 program with a grid box of 60 × 60 × 60 Å that was generated around the substrate binding site of SrtA. Ligand-receptor docking was performed with the Autodock4 program using the Lamarckian genetic algorithm, and the Pseudo-Solis and Wets algorithm was applied for the local search. Each docking was performed 20 times, yielding 50 docked conformations. The other settings were the default parameters. The docking graphs were prepared in PyMol 2.3.

FITC-IgG binding to staphylococci. Overnight cultures of wild-type and Δ*srtA* mutant *S. aureus* Newman strains were diluted 1:1000 with TSB and cultured at 37 °C in the presence of the inhibitors at different concentrations until A_{600} reached 1.0. The bacteria were centrifuged and rinsed three times with PBS and subsequently suspended in PBS supplemented with 4 μL of FITC-IgG antibody (eBioscience) for 30

min at rt. The *S. aureus* was centrifuged, suspended in PBS, and washed three times. The fluorescence intensity was monitored using Flex Station 3 (Molecular Devices) at emission and excitation wavelengths of 495 and 520 nm, respectively. Each data point was measured in three technical replicates, and three independent experiments were performed on each compound.

Western blot. Overnight cultures of *S. aureus* Newman were diluted 1:1000 and further cultured at 37 °C with different concentrations of the inhibitors until A_{600} reached 3.0. The bacteria were rinsed three times with PBS and subsequently resuspended in PBS supplemented with 1 μL of 5 mg/mL lysozyme and incubated at 37 °C for 30 min. After centrifugation, the protoplasts were precipitated, and the supernatants (cell wall-anchored proteins) were collected. Aliquots were resolved and separated using SDS-PAGE, and the cell wall-anchored SpA protein was analyzed by immunoblotting. The cytoplasmic protein ClpP of *S. aureus* was used as the loading control. Three independent experiments were performed.

Biofilm formation. Overnight cultures of the *S. aureus* strains were diluted 1:100 with fresh TSB medium. Two hundred microliters of the diluted cultures were added in quadruplicate to the wells of 96-well microtiter plates (Cell Biolabs) with different concentrations of inhibitors. After incubation under static culture conditions at 37 °C for 18 hr, the medium was removed, and the wells were carefully rinsed three times with PBS. Subsequently, the dried and fixed biofilms of the bacteria were stained with 0.1% (w/v) crystal violet solution for 15 min. Excess stain was discarded, and the plates were washed three times with sterile distilled water and photographed. For

quantification, 30% (v/v) acetic acid solution was used to dissolve the crystal violet stain, and the absorbance was measured at 595 nm using a microplate reader. Three independent experiments were performed on each compound.

Antiinfection of *S. aureus* USA300 in a mouse model. Lethal challenge experiments were performed at the Shanghai Public Health Clinical Center following animal care and use protocols that were reviewed, approved, and supervised by the Committee for Animal Experiments at Fudan University. Overnight cultures of *S. aureus* USA300 were diluted 1:1,000 into 30 mL of fresh TSB and grown with rotation at 37 °C for 3 hr. The bacteria were centrifuged at 3,000 g, washed, and suspended in PBS to A_{600} 0.8 or 1.6. BALB/c mice (6-week-old females) were randomly assigned into two cohorts. Water and laboratory chow were provided ad libitum. **TD** was suspended in ddH_2O in the presence of 4% Tween 80 and 4% DMSO and administered by i.p. injection at a dose of 40 mg/kg at 24 hr intervals. Four hours after the first injection of compound **TD** or saline (placebo), mice were challenged by periorbital injection of *S. aureus* USA300. Aliquots of the inoculum were plated and the CFUs were counted. Animals were monitored for survival for a 10-day observation period. The log-rank test was used to analyze the mortality data; $P < 0.05$ was deemed statistically significant.

ASSOCIATED CONTENT

Supporting Information

The Supporting Information is available free of charge on the ACS Publications

website at DOI:

Additional figures and analytical data for target compounds (PDF)

Molecular formula strings and biological data (CSV)

AUTHOR INFORMATION

Corresponding Author

*jhzx.msm@gmail.com (S.Y.); *yangcg@simm.ac.cn (C.-G.Y.)

Author Contributions

§ T.Y. and T.Z. contributed equally to this work. C.-G.Y. and S.Y. conceived the project. C.-G.Y. designed the research and wrote the paper with help from T.Y. and T.Z. T.Y. performed the biological annotation with help from X.G. and L.L. T.Z. and Z.D. synthesized the compounds. All the authors reviewed the results and approved the manuscript.

Notes

The authors declare no competing financial interests.

ACKNOWLEDGMENTS

This study was supported by the National Natural Science Foundation of China (81861138046 and 21725801) and the Science and Technology Commission of Shanghai Municipality (17XD1404400).

ABBREVIATIONS

CD, circular dichroism; CFU, colony-forming unit; FRET, fluorescence resonance energy transfer; HTS, high-throughput screening; MIC, minimal inhibitory concentration; MTSET, N,N,N-trimethyl-2-[(methylsulfonyl)sulfanyl]ethanaminium bromide; MRSA, methicillin-resistant *S. aureus*; PAINS, panassay interference compound; PBS, phosphate-buffered saline; SAR, structure-activity relationship; SrtA, sortase A; TD, tideglusib; TLC, thin-layer chromatography; TSB, tryptic soy broth.

REFERENCES

(1). Lowy, F. D. *Staphylococcus aureus* infections. *N. Engl. J. Med.* **1998,** *339*, 520-532.

(2). Diekema, D. J.; Pfaller, M. A.; Schmitz, F. J. Survey of infections due to *Staphylococcus* species: frequency of occurrence and antimicrobial susceptibility of isolates collected in the United States, Canada, Latin America, Europe, and the Western Pacific region for the SENTRY Antimicrobial Surveillance Program, 1997-1999. *Clin. Infect. Dis.* **2001,** *32*, 114-132.

(3). Turner, N. A.; Sharma-Kuinkel, B. K.; Maskarinec, S. A.; Eichenberger, E. M.; Shah, P. P.; Carugati, M.; Holland, T. L.; Fowler, V. G., Jr. Methicillin-resistant *Staphylococcus aureus*: an overview of basic and clinical research. *Nat. Rev. Microbiol.* **2019,** *17*, 203-218.

(4). Chambers, H. F.; Deleo, F. R. Waves of resistance: *Staphylococcus aureus* in the antibiotic era. *Nat. Rev. Microbiol.* **2009,** *7*, 629-641.

(5). Stryjewski, M. E.; Corey, G. R. Methicillin-resistant *Staphylococcus aureus*: an evolving pathogen. *Clin. Infect. Dis.* **2014,** *58*, 10-19.

(6). Fischbach, M. A.; Walsh, C. T. Antibiotics for emerging pathogens. *Science* **2009,** *325*, 1089-1093.

(7). Zhou, L. L.; Yang, C. G. Chemical intervention on *Staphylococcus aureus* virulence. *Chin. J. Chem.* **2019,** *37*, 183-193.

(8). Totsika; Makrina. Disarming pathogens: benefits and challenges of antimicrobials that target bacterial virulence instead of growth and viability. *Future Med. Chem.* **2017,** *9*, 267-269.

(9). Dickey, S. W.; Cheung, G. Y. C.; Otto, M. Different drugs for bad bugs: antivirulence strategies in the age of antibiotic resistance. *Nat. Rev. Drug Discov.* **2017,** *16*, 457-471.

(10). Lakemeyer, M.; Zhao, W.; Mandl, F. A.; Hammann, P.; Sieber, S. A. Thinking outside the box-novel antibacterials to tackle the resistance crisis. *Angew. Chem. Int. Ed. Engl.* **2018,** *57*, 14440-14475.

(11). Wu, S. C.; Liu, F.; Zhu, K.; Shen, J. Z. Natural products that target virulence factors in antibiotic-resistant *Staphylococcus aureus*. *J. Agric. Food. Chem.* **2019,** *67*, 13195-13211.

(12). Mazmanian, S. K.; Liu, G.; Jensen, E. R.; Lenoy, E.; Schneewind, O. *Staphylococcus aureus* Sortase mutants defective in the display of surface proteins and in the pathogenesis of animal infections. *Proc. Natl. Acad. Sci. U. S. A.* **2000,** *97*, 5510-5515.

(13). Weiss, W. J.; Lenoy, E.; Murphy, T.; Tardio, L.; Burgio, P.; Projan, S. J.; Schneewind, O.; Alksne, L. Effect of srtA and srtB gene expression on the virulence of

Staphylococcus aureus in animal models of infection. *J. Antimicrob. Chemother.* **2004,** *53*, 480-486.

(14). Siegel, S. D.; Reardon, M. E.; Ton-That, H. Anchoring of LPXTG-like proteins to the gram-positive cell wall envelope. *Curr. Top. Microbiol. Immunol.* **2017,** *404*, 159-175.

(15). Mazmanian, S. K.; Liu, G.; Ton-That, H. *Staphylococcus aureus* Sortase, an enzyme that anchors surface proteins to the cell wall. *Science* **1999,** *285*, 760-762.

(16). Cheng, A. G.; Kim, H. K.; Burts, M. L.; Krausz, T.; Schneewind, O.; Missiakas, D. M. Genetic requirements for *Staphylococcus aureus* abscess formation and persistence in host tissues. *FASEB J.* **2009,** *23*, 3393-3404.

(17). Cascioferro, S.; Raffa, D.; Maggio, B.; Raimondi, M. V.; Schillaci, D.; Daidone, G. Sortase A inhibitors: recent advances and future perspectives. *J. Med. Chem.* **2015,** *58*, 9108-9123.

(18). Si, L.; Li, P.; Liu, X.; Luo, L. Chinese herb medicine against Sortase A catalyzed transformations, a key role in gram-positive bacterial infection progress. *J. Enzyme Inhib. Med. Chem.* **2016,** *31*, 184-196.

(19). Won, T. H.; Song, I. H.; Kim, K. H.; Yang, W. Y.; Lee, S. K.; Oh, D. C.; Oh, W. K.; Oh, K. B.; Shin, J. Bioactive Metabolites from the Fruits of Psoralea corylifolia. *J. Nat. Prod.* **2015,** *78*, 666-673.

(20). Zhang, B.; Teng, Z.; Li, X.; Lu, G.; Deng, X.; Niu, X.; Wang, J. Chalcone attenuates *Staphylococcus aureus* virulence by targeting Sortase A and α-hemolysin. *Front. Microbiol.* **2017,** *8*, 1715.

(21). Wang, J.; Song, M.; Pan, J.; Shen, X.; Liu, W.; Zhang, X.; Li, H.; Deng, X. Quercetin impairs *Streptococcus pneumoniae* biofilm formation by inhibiting sortase A activity. *J. Cell. Mol. Med.* **2018,** *22*, 6228-6237.

(22). Mu, D.; Luan, Y.; Wang, L.; Gao, Z.; Yang, P.; Jing, S.; Wang, Y.; Xiang, H.; Wang, T.; Wang, D. The combination of salvianolic acid A with latamoxef completely protects mice against lethal pneumonia caused by methicillin-resistant *Staphylococcus aureus*. *Emerg. Microbes. Infect.* **2020,** *9*, 169-179.

(23). Wang, L.; Bi, C.; Cai, H.; Liu, B.; Zhong, X.; Deng, X.; Wang, T.; Xiang, H.; Niu, X.; Wang, D. The therapeutic effect of chlorogenic acid against *Staphylococcus aureus* infection through sortase A inhibition. *Front. Microbiol.* **2015,** *6*, 1031.

(24). Oh, K. B.; Kim, S. H.; Lee, J.; Cho, W. J.; Lee, T.; Kim, S. Discovery of diarylacrylonitriles as a novel series of small molecule Sortase A inhibitors. *J. Med. Chem.* **2004,** *47*, 2418-2421.

(25). Cascioferro, S.; Parrino, B.; Carbone, D.; Schillaci, D.; Giovannetti, E.; Cirrincione, G.; Diana, P. Thiazoles, their benzofused systems, and thiazolidinone derivatives: versatile and promising tools to combat antibiotic resistance. *J. Med. Chem.* **2020**, DOI: 10.1021/acs.jmedchem.1029b01245.

(26). Chan, A. H.; Yi, S. W.; Weiner, E. M.; Amer, B. R.; Sue, C. K.; Wereszczynski, J.; Dillen, C. A.; Senese, S.; Torres, J. Z.; McCammon, J. A.; Miller, L. S.; Jung, M. E.; Clubb, R. T. NMR structure-based optimization of *Staphylococcus aureus* sortase A pyridazinone inhibitors. *Chem. Biol. Drug. Des.* **2017,** *90*, 327-344.

(27). Lee, Y. J.; Han, Y. R.; Park, W.; Nam, S. H.; Oh, K. B.; Lee, H. S. Synthetic analogs

of indole-containing natural products as inhibitors of sortase A and isocitrate lyase. *Bioorg. Med. Chem. Lett.* **2010,** *20*, 6882-6885.

(28). Wehrli, P. M.; Uzelac, I.; Olsson, T.; Jacso, T.; Tietze, D.; Gottfries, J. Discovery and development of substituted thiadiazoles as inhibitors of *Staphylococcus aureus* Sortase A. *Bioorg. Med. Chem.* **2019,** *27*, 115043.

(29). Gosschalk, J. E.; Chang, C.; Sue, C. K.; Siegel, S. D.; Wu, C.; Kattke, M. D.; Yi, S. W.; Damoiseaux, R.; Jung, M. E.; Ton-That, H.; Clubb, R. T. A cell-based screen in actinomyces oris to identify Sortase inhibitors. *Sci. Rep.* **2020,** *10*, 8520.

(30). Rentero Rebollo, I.; McCallin, S.; Bertoldo, D.; Entenza, J. M.; Moreillon, P.; Heinis, C. Development of protent and selective *S. aureus* Sortase A inhibitors based on peptide macrocycles. *ACS Med. Chem. Lett.* **2016,** *7*, 606-611.

(31). Wang, J.; Li, H.; Pan, J.; Dong, J.; Zhou, X.; Niu, X.; Deng, X. Oligopeptide targeting Sortase A as potential anti-infective therapy for *Staphylococcus aureus*. *Front. Microbiol.* **2018,** *9*, 245.

(32). Scott, C. J.; McDowell, A.; Martin, S. L.; Lynas, J. F.; Vandenbroeck, K.; Walker, B. Irreversible inhibition of the bacterial cysteine protease-transpeptidase sortase (SrtA) by substrate-derived affinity labels. *Biochem. J.* **2002,** *366*, 953-958.

(33). Kruger, R. G.; Barkallah, S.; Frankel, B. A.; McCafferty, D. G. Inhibition of the *Staphylococcus aureus* sortase transpeptidase SrtA by phosphinic peptidomimetics. *Bioorg. Med. Chem.* **2004,** *12*, 3723-3729.

(34). Jackson, P. A.; Widen, J. C.; Harki, D. A.; Brummond, K. M. Covalent modifiers: a chemical perspective on the reactivity of α, β-unsaturated carbonyls with thiols via

hetero-michael addition reactions. *J. Med. Chem.* **2017,** *60*, 839-885.

(35). Jaudzems, K.; Kurbatska, V.; Je Kabsons, A.; Bobrovs, R.; Rudevica, Z.; Leonchiks, A. Targeting bacterial Sortase A with covalent inhibitors: 27 new starting points for structure-based hit-to-lead optimization. *ACS Infect. Dis.* **2020,** *6*, 186-194.

(36). Hou, X.; Wang, M.; Wen, Y.; Ni, T.; Guan, X.; Lan, L.; Zhang, N.; Zhang, A.; Yang, C. G. Quinone skeleton as a new class of irreversible inhibitors against *Staphylococcus aureus* Sortase A. *Bioorg. Med. Chem. Lett.* **2018,** *28*, 1864-1869.

(37). Barthels, F.; Marincola, G.; Marciniak, T.; Konhauser, M.; Hammerschmidt, S.; Bierlmeier, J.; Distler, U.; Wich, P. R.; Tenzer, S.; Schwarzer, D.; Ziebuhr, W.; Schirmeister, T. Asymmetric disulfanylbenzamides as irreversible and selective inhibitors of *Staphylococcus aureus* Sortase A. *ChemMedChem* **2020,** *15*, 839-850.

(38). Zhang, J.; Liu, H.; Zhu, K.; Gong, S.; Dramsi, S.; Wang, Y. T.; Li, J.; Chen, F.; Zhang, R.; Zhou, L.; Lan, L.; Jiang, H.; Schneewind, O.; Luo, C.; Yang, C. G. Antiinfective therapy with a small molecule inhibitor of *Staphylococcus aureus* Sortase. *Proc. Natl. Acad. Sci. U. S. A.* **2014,** *111*, 13517-13522.

(39). Study of tideglusib in adolescent and adult patients with myotonic dystrophy (NCT02858908). *ClinicalTrials. gov Web Site* **2016**, https://clinicaltrials.gov/ct2/show/NCT02858908 (accessed April 02852020).

(40). Martinez, A. First non-ATP competitive glycogen synthase kinase 3β (GSK-3β) inhibitors : thiadiazolidinones (TDZD) as potential drugs for the treatment of alzheimer's disease. *J. Med. Chem.* **2002,** *45*, 1292-1299.

(41). Turner, E. M.; Blazer, L. L.; Neubig, R. R.; Husbands, S. M. Small molecule

inhibitors of regulator of G protein signalling (RGS) proteins. *ACS Med. Chem. Lett.* **2012,** *3*, 146-150.

(42). Marcinkeviciene, J.; Rogers, M. J.; Kopcho, L.; Jiang, W.; Wang, K.; Murphy, D. J.; Lippy, J.; Link, S.; Chung, T. D. Y.; Hobbs, F.; Haque, T.; Trainor, G. L.; Slee, A.; Stern, A. M.; Copeland, R. A. Selective inhibition of bacterial dihydroorotate dehydrogenases by thiadiazolidinediones. *Biochem. Pharmacol.* **2000,** *60*, 339-342.

(43). Emma Jane Smith; Livia Visai; Kerrigan，, S. W.; Pietro Speziale; Foster, T. J. The Sbi Protein Is a Multifunctional Immune Evasion Factor of *Staphylococcus aureus*. *Infect. Immun.* **2011,** *Sept*, 3801-3809.

(44). Dominguez, J. M.; Fuertes, A.; Orozco, L.; del Monte-Millan, M.; Delgado, E.; Medina, M. Evidence for irreversible inhibition of glycogen synthase kinase-3β by tideglusib. *J. Biol. Chem.* **2012,** *287*, 893-904.

(45). Blazer, L. L.; Zhang, H.; Casey, E. M.; Husbands, S. M.; Neubig, R. R. A nanomolar-potency small molecule inhibitor of regulator of G protein signaling proteins. *Biochem.* **2011,** *50*, 3181-3192.

(46). Boschi, D.; Pippione, A. C.; Sainas, S.; Lolli, M. L. Dihydroorotate dehydrogenase inhibitors in anti-infective drug research. *Eur. J. Med. Chem.* **2019,** *183*, 111681.

(47). Suree, N.; Liew, C. K.; Villareal, V. A.; Thieu, W.; Fadeev, E. A.; Clemens, J. J.; Jung, M. E.; Clubb, R. T. The structure of the *Staphylococcus aureus* sortase-substrate complex reveals how the universally conserved LPXTG sorting signal is recognized. *J. Biol. Chem.* **2009,** *284*, 24465-24477.

(48). Ilangovan, U.; Ton-That, H.; Iwahara, J.; Schneewind, O.; Clubb, R. T. Structure

of Sortase, the transpeptidase that anchors proteins to the cell wall of *Staphylococcus aureus*. *Proc. Natl. Acad. Sci. U. S. A.* **2001,** *98*, 6056-6061.

(49). Pouliot, M.; Jeanmart, S. Pan assay interference compounds (PAINS) and other promiscuous compounds in antifungal research. *J. Med. Chem.* **2016,** *59*, 497-503.

(50). Aldrich, C.; Bertozzi, C.; Georg, G. I.; Kiessling, L.; Lindsley, C.; Liotta, D.; Merz, K. M., Jr.; Schepartz, A.; Wang, S. The ecstasy and agony of assay interference compounds. *J. Med. Chem.* **2017,** *60*, 2165-2168.

(51). Mazmanian, S. K.; Ton-That, H.; Su, K.; Schneewind, O. An Iron-regulated sortase anchors a class of surface protein during *Staphylococcus aureus* pathogenesis. *Proc. Natl. Acad. Sci. U. S. A.* **2002,** *99*, 2293-2298.

(52). Falugi, F.; Kim, H. K.; Missiakas, D. M.; Schneewind, O. Role of protein A in the evasion of host adaptive immune responses by *Staphylococcus aureus*. *mBio.* **2013,** *4*, e00575-00513.

(53). Ton-That, H.; Mazmanian, S. K.; Alksne, L.; Schneewind, O. Anchoring of surface proteins to the cell wall of *Staphylococcus aureus*. Cysteine 184 and histidine 120 of sortase form a thiolate-imidazolium ion pair for catalysis. *J. Biol. Chem.* **2002,** *277*, 7447-7452.

(54). Otto, M. *Staphylococcal* biofilms. *Curr. Top. Microbiol. Immunol.* **2008,** *322*, 207-228.

(55). Saini, N. K.; Suresh, P. S.; Lella, M.; Bhamidipati, R. K.; Rajagopal, S.; Mullangi, R. LC–MS/MS determination of tideglusib, a novel GSK-3β inhibitor in mice plasma and its application to a pharmacokinetic study in mice. *J. Pharm. Biomed. Anal.* **2018,** *148*,

100-107.

Table of Contents graphic

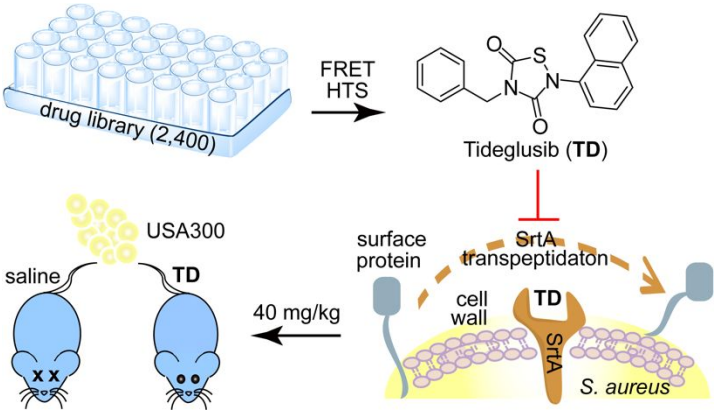

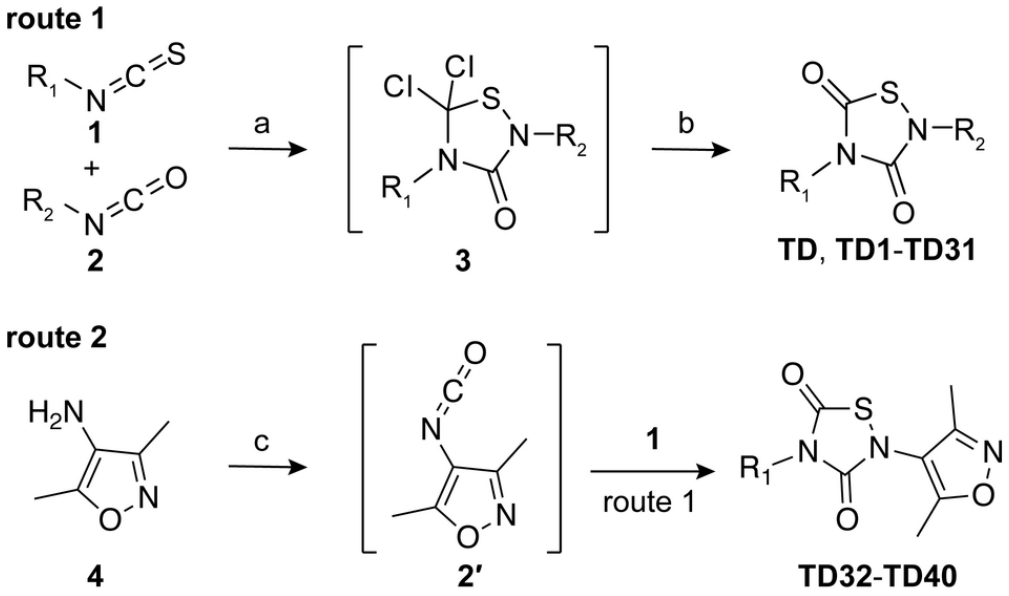

Scheme 1

80x48mm (300 x 300 DPI)

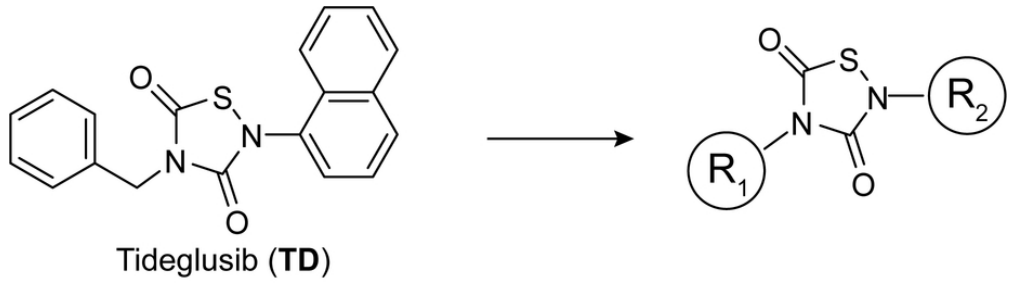

Figure 1

78x21mm (300 x 300 DPI)

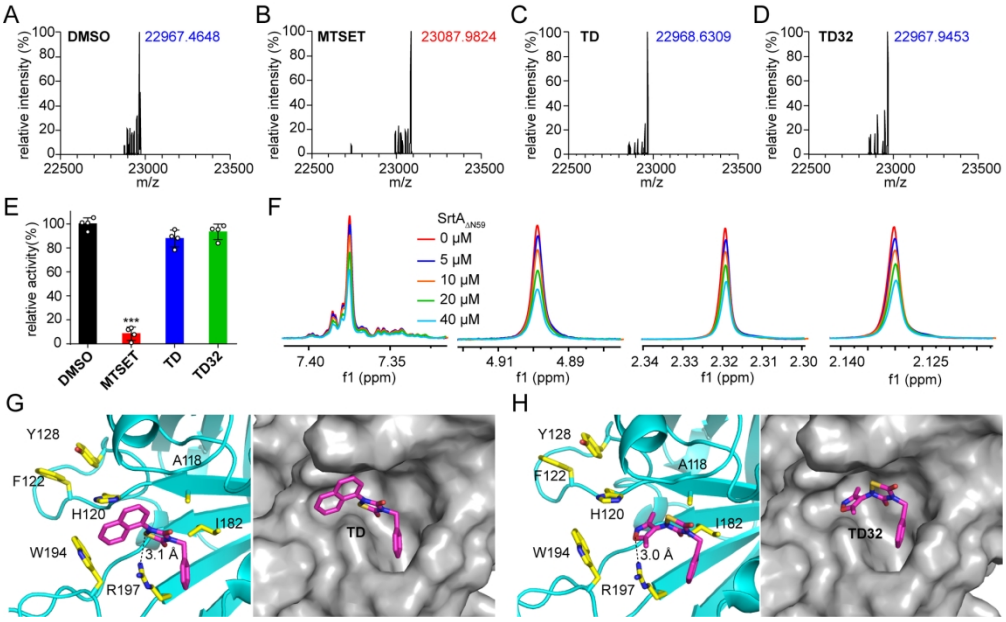

Figure 2

173x106mm (300 x 300 DPI)

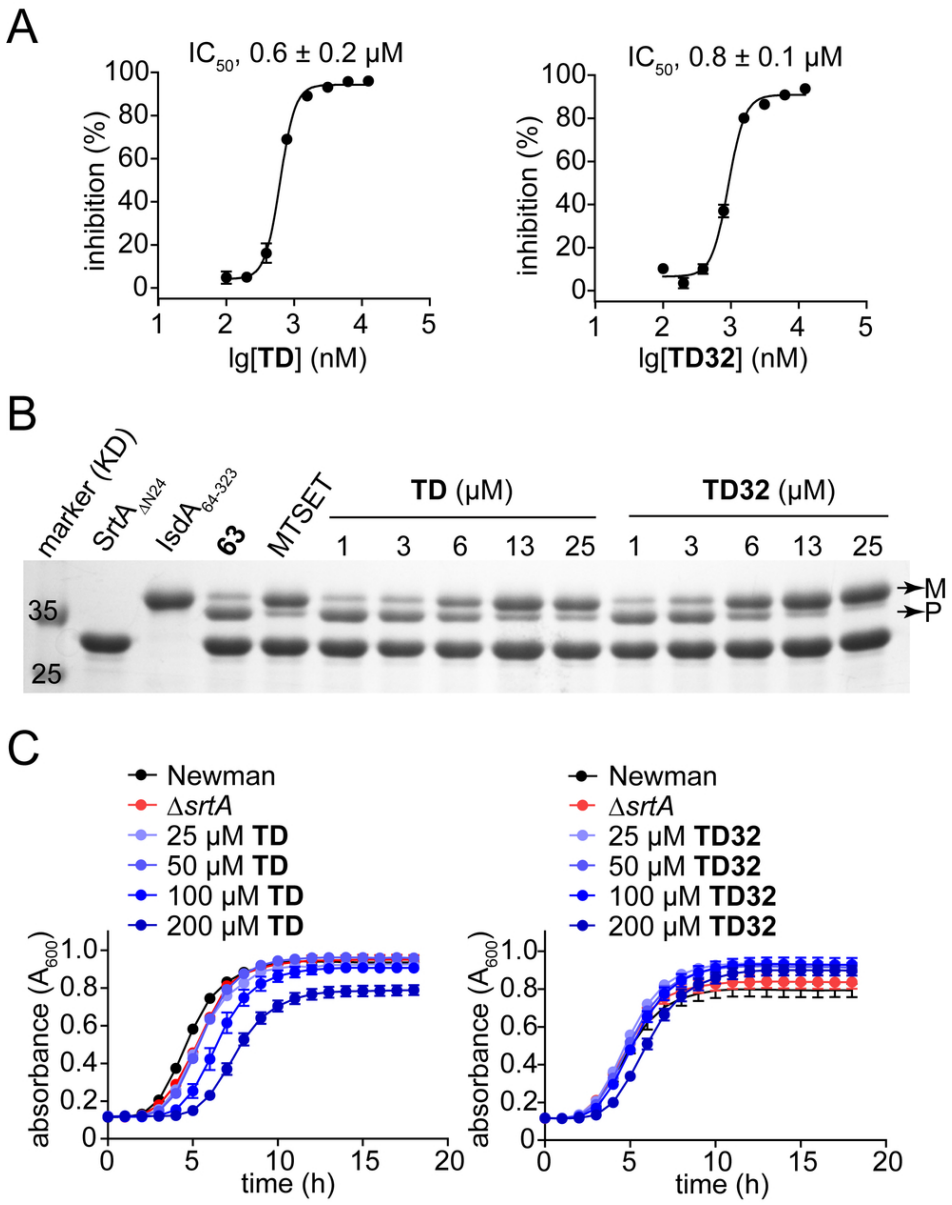

Figure 3

83x106mm (300 x 300 DPI)

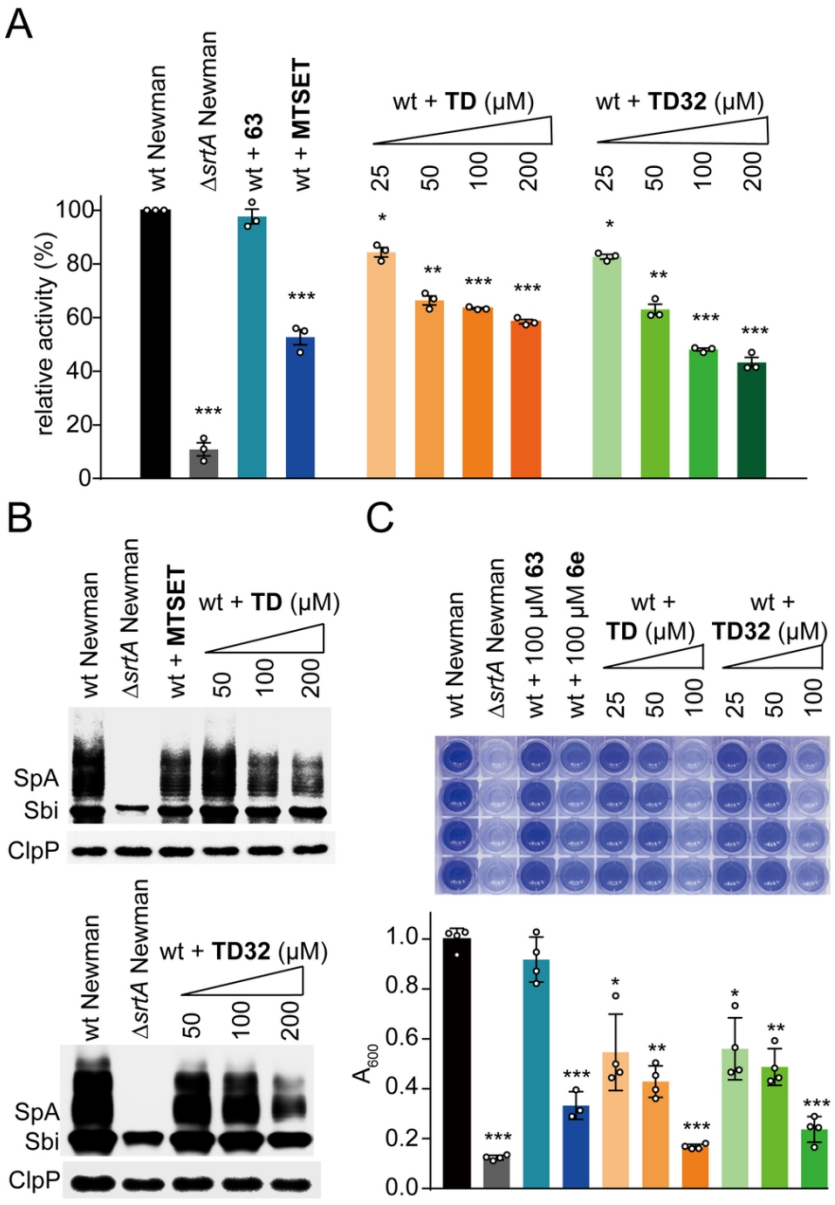

Figure 4

84x121mm (300 x 300 DPI)

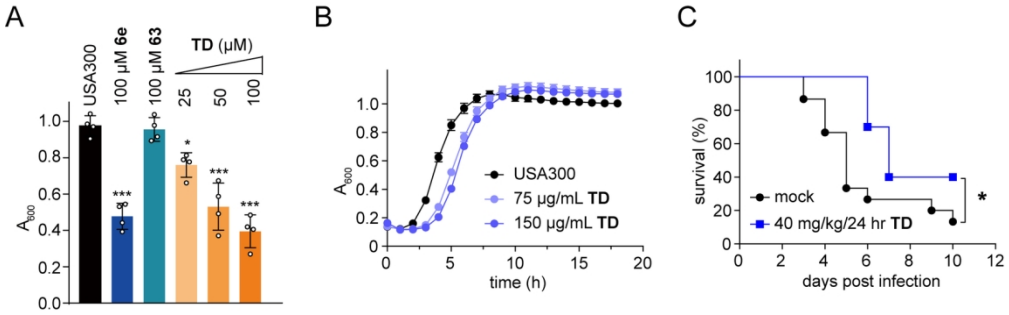

Figure 5

148x46mm (300 x 300 DPI)